NOVA SCHOOL OF SCIENCE & TECHNOLOGY

DEPARTMENT OF LIFE SCIENCES

ANDRÉ JORGE BALSINHA

BSc in Biochemistry

EXPLORING THE DNA DAMAGE RESPONSE IN SKELETAL MUSCLE CELLS

MASTER IN MOLECULAR GENETICS AND BIOMEDICINE

NOVA University Lisbon

September, 2023

NOVA SCHOOL OF
SCIENCE & TECHNOLOGY

DEPARTMENT OF
LIFE SCIENCES

EXPLORING THE DNA DAMAGE RESPONSE IN SKELETAL MUSCLE CELLS

ANDRÉ JORGE BALSINHA

BSc in Biochemistry

Adviser: Sérgio Fernandes de Almeida
Group Leader, iMM-JLA and Associate Professor, FMUL

Co-adviser: Ana Rita Grosso
Assistant Professor, NOVA School of Science and Technology

Examination Committee

Chair: Alexandra R. Fernandes
Associate Professor, NOVA School of Science and Technology

Rapporteur: Silvia Di Francescantonio
Senior Postdoctoral Researcher, iMM-JLA

Member: Sérgio Fernandes de Almeida
Group Leader, iMM-JLA and Associate Professor, FMUL

MASTER IN MOLECULAR GENETICS AND BIOMEDICINE

NOVA University Lisbon
September, 2023

Exploring the DNA Damage Response in skeletal muscle cells

This document was created with the (pdf/Xe/Lua)LaTeX processor and the NOVAthesis template (v7.0.2) [1].

Acknowledgements

Firstly, I would like to thank my adviser, Professor Sérgio de Almeida, for accepting me and trusting me with this position in his lab. With this opportunity, I was able to be around an environment of exciting work and amazing researchers. I was also able to learn the reality of the world of science and develop critical thinking and resilience, thus turning myself into a better researcher as well as a better person.

Additionally, I also want to thank my supervisor Professor Ana Rita Grosso, for taking the responsibility and allowing me to be part of this project.

I would also like to thank the BioImaging unit from iMM, for the patience, sympathy and always helping when needed when the work requested.

To the person who deserves the most acknowledgments in this project, I would like to give special thanks to Inês. Thank you for taking me under your wing and having the patience that you had to have for my inexperience and for all the hours that you invested in me. I also thank you for letting me be part of your work, even though this is my master's project, I truly did everything that I could for you too because you deserve it. Thank you for showing me how a great person deals with science and life, and for showing me that there are people that truly love what they do. I will take everything that you taught me from now on. Thank you for being a great boss and a better friend.

To all SAlmeida lab, Cris, Madalena, Robert, Anne-Valerie, Anna, Bilal, and Margarida who took me as one of their own since day 1 and taught me every time that I needed. All the moments that we shared in the lab were amazing and did not even feel like work. A special thanks to Rita and Ian, who besides being great co-workers, were the ones who had to deal with all my problems, stresses, and bad jokes all the time. These for sure will be friendships that I will take for life.

To Vitorino and Rebelo, who were the ones who shared with me this experience of making a master's degree in such a difficult course. Thank you for making it easier by always putting a smile on my face.

Thank you also Hugo, Diogo, Catarina and Bento. It is easy to deal with people in a short amount of time, but you already know me for a few years now so I must be a decent guy to be around. Like always you made this journey easier. It always feels nice to be able

to be with you after a hard day of work.

Finalmente, gostaria de agradecer à minha família. Escusado será dizer que vocês são a base do meu sucesso. Todo o esforço que eu meto no meu trabalho e no meu futuro só foi possível porque vocês sacrificaram tudo o que podiam. Obrigado pela confiança de me deixarem seguir o que eu gosto sem nunca questionar. Obrigado por saber que sempre estarão lá não importa se eu erre ou não. Se eu não consegui mais, foi porque não consegui. Não vos irei desiludir.

Ao Tepi, por ser o meu melhor amigo desde que comecei esta aventura.

Portion of this dissertation results are published in a peered-review journal [2].

”

“My average self, do you really have time to look down like that?”

— Ryūnosuke Tanaka

Abstract

One of the most dominant phenotypes of aging and many diseases is the low efficiency for muscle regeneration, so it is crucial to better understand its mechanism. Skeletal muscle cells cannot replicate upon being terminally differentiated. When they get mechanically injured, they are capable of regenerating by activating and recruiting nearby satellite cells. These will differentiate and fuse with the damaged fiber. However, the muscle cells are also prone to DNA damage caused by different sources. How myofibers repair themselves upon DNA damage is still poorly studied. We believe that muscle cells also activate satellite cells upon DNA damage, the same way that it happens upon injury. In this work, not only it was reinforced the hypothesis that muscle cells use a novel mechanism to eliminate DNA damage, but it was also tested if the muscle resorted to satellite cell activation to repair the damaged fibers. We started by analyzing the cytoplasm of DNA-damaged myotubes by Electron Microscopy and identified a higher level of vesicles when compared to wild-type myotubes. We also analyzed the conditioned medium of the same cells by Mass Spectrometry. Finally, we tested if myoblasts would activate upon being in contact with the conditioned medium, by seeing the expression of various differentiation markers and testing several techniques. The results suggest that there might be activation of satellite cells due to DNA damage.

Keywords: DNA damage, Muscle cells, DNA Damage Response, Satellite cells

Resumo

Um dos principais fenótipos característico do envelhecimento e de muitas doenças é a perda de eficácia da regeneração dos músculos, o que faz com que seja indispensável entender mais sobre este mecanismo. As células do músculo esquelético não são capazes de replicar após serem diferenciadas. Por contrapartida, quando estas são danificadas, são capazes de regenerar devido à ativação e recrutamento de células satélite. Estas vão diferenciar e fundir com a fibra muscular danificada. Porém, a maneira com que as fibras musculares são capazes de regenerar devido a dano no ADN ainda não está bem esclarecido. Acreditamos que as células do músculo após sofrerem dano no ADN também ativam células satélite, da mesma forma que acontece com as lesões no músculo. Neste trabalho, não só foi reforçado a hipótese de que as células musculares utilizam um mecanismo ainda não reportado para a eliminação do ADN danificado, como se tentou confirmar que as células satélite são ativadas para reparar as fibras musculares. Começou-se por analisar o citoplasma de miotubos com o ADN danificado por Microscopia Eletrónica e identificou-se um maior número de vesículas quando em comparação com miotubos normais. O meio condicionado destas células também foi analisado por Espectrometria de Massa. Por último, foi testado se os mioblastos são capazes de diferenciar após serem tratados com o meio condicionado de miotubos danificados. Para isso, analisou-se a expressão de diversos biomarcadores de diferenciação usando diversas técnicas. Os resultados sugerem que possa existir ativação de células satélite devido ao dano no ADN.

Palavras-chave: Dano do ADN, Células musculares, Resposta ao dano do ADN, Células Satélite

Contents

List of Figures

List of Tables

Acronyms

53BP1 53-Biding Protein 1 *(p. 3)*

a-EJ Alternative End-joining *(p. 5)*
AMPK AMP-activated Kinase *(p. 11)*
AP Apurinic/apyrimidinic *(p. 2)*
APLF Aprataxin-and-PNK-like Factor *(p. 3)*
AR Always Renewed *(p. 16)*
ATG Autophagy-related *(p. 12)*
ATM Ataxia Telangectasia Mutated *(p. 3)*
ATMi Ataxia Telangectasia Mutated inhibitor *(p. 16)*
ATR Ataxia Telangiectasia and Rad3 related *(p. 3)*

BER Base Excision Repair *(pp. 2, 9)*
BRCA1 Breast Cancer Type 1 *(p. 3)*
BRCA2 Breast Cancer Type 2 *(p. 3)*

cDNA complementary DNA *(p. 18)*
CM Conditioned Medium *(p. 16)*
CPDs Cyclobutane Pyrimidine Dimers *(p. 2)*

DAPI 4,6-diamidino-2-phenylindole *(p. 19)*
DASP DNA Damage-Associated Secretory Phenotype *(p. 13)*
DDR DNA Damage Response *(pp. 2, 3, 9–11, 13)*
DMD Duchenne Muscular Dystrophy *(p. 10)*
DNA Deoxyribonucleic Acid *(p. 1)*
DNA-PKcs DNA-dependent Protein Kinase catalytic subunits *(p. 3)*
DSB Double Strand Break *(pp. 2–5, 11)*
DTT Dithiothreitol *(p. 16)*

ECM Extracellular Matrix *(p. 8)*
EDMD Emery–Dreifuss Muscular Dystrophy *(p. 10)*
EM Electron Microscopy *(pp. 13, 20)*
ER Endoplasmic Reticulum *(p. 9)*
ERK1/2 Extracellular Signal-regulated Kinase 1/2 *(p. 42)*
ESI Electrospray Ionization *(p. 21)*
Exo1 Exonuclease 1 *(p. 3)*

FCS Fetal Calf Serum *(p. 42)*
FGF6 Fibroblast Growth Factor 6 *(p. 8)*
FI Fusion Index *(pp. 16, 19)*
FSHD Facio-Scapulohumeral Dystrophy *(p. 11)*

GFR Growth Factor Reduced *(p. 15)*

HGF Hepatocyte Growth Factor *(p. 8)*
HR Homologous Recombination *(pp. 3, 5, 10)*
HRP Horseradish Peroxidase *(p. 17)*
HU Hydroxyurea *(p. 2)*

IF Immunofluorescence *(pp. 14, 19)*
IGF-1 Insulin-like Growth Factor 1 *(p. 8)*

LC Liquid Chromatography *(p. 20)*
LC3 Light Chain 3 *(p. 12)*
LGMD Limb Girdle Muscular Dystrophies *(p. 10)*

MAPK Mitogen-Activated Protein Kinase *(p. 42)*
MMR DNA Mismatch Repair *(p. 2)*
MRF Myogenic Regulatory Factors *(p. 6)*
MRN Mre11-Rad50-Nbs1 *(p. 3)*
MS Mass Spectrometry *(p. 20)*
mTOR Mammalian target of rapamycin *(p. 11)*
MyH3 Myosin Heavy Chain 3 *(p. 14)*
MyHC Myosin Heavy Chain *(p. 7)*
MyoB Myoblasts *(p. 6)*
MyoT Myotubes *(p. 6)*

NCS Neocarzinostatin *(pp. 2, 3, 16)*
NER Nucleotide Excision Repair *(pp. 2, 10)*

Net39 Nuclear envelope transmembrane protein 39 *(p. 10)*
NHEJ Non-Homologous End Joining *(pp. 3, 4, 10)*
NO Nitric Oxide *(p. 8)*
NR No Renewed *(p. 16)*

o/n overnight *(p. 17)*
OPLS-DA Orthogonal Partial Least Squares Discriminant Analysis *(p. 21)*
OsO_4 Osmium tetroxide *(p. 20)*

Pax3 Paired-box protein 3 *(p. 6)*
Pax7 Paired-box protein 7 *(p. 6)*
PBS Phosphate-buffered Saline *(p. 15)*
PCA Principal Components Analysis *(p. 21)*
PCR Polymerase Chain Reaction *(p. 17)*
PDGF-B Platelet Derived Growth Factor subunit B *(p. 8)*
PFA Paraformaldehyde *(p. 20)*
PI3KC3 Phosphatidylinositol 3-kinase Class III *(p. 11)*
PI3P Phosphatidylinositol 3-phosphate *(p. 11)*
PIKK Phosphatidylinositol 3-Kinase-related Kinase *(p. 3)*
PLS-DA Partial Least Squares Discriminant Analysis *(p. 21)*

RFP Replication Fork Pause *(p. 1)*
ROS Reactive Oxygen Species *(pp. 1, 8, 9, 11)*
RPA Replication Protein A *(p. 3)*
RT Room Temperature *(p. 16)*
RT-qPCR Reverse Transcriptase quantitative Polymerase Chain Reaction *(pp. 14, 17)*

SAE2 SUMO-activating Enzyme subunit 2 *(p. 3)*
SDS Sodium Dodecyl Sulfate *(p. 16)*
SDS-PAGE SDS-Polyacrylamide Gel Electrophoresis *(p. 17)*
SNARE Snap Receptor *(p. 12)*
SSB Single Strand Break *(p. 2)*

TCR Transcription-Coupled Repair *(p. 10)*
TGF-b Transforming Growth Factor-beta *(p. 8)*

UPLC Ultra Performance Liquid Chromatography *(p. 21)*
UPLC-MS Ultra Performance Liquid Chromatography–Mass Spectrometry *(p. 14)*

VIP Variable Importance in Projection *(pp. 21, 23)*

WB Western Blot *(pp. 14, 16)*

WRN Werner *(p. 3)*

XRCC4 X-ray Repair Cross-Complementing protein *(p. 3)*

1 Introduction

1.1 DNA damage

All organisms possess in their cells genetic information in the form of Deoxyribonucleic Acid (DNA). This molecule works as a code that translates all the information to physical attributes, thus influencing the organism's growth as well as its function. So it is crucial that the DNA has to maintain its integrity to keep the cell system well regulated. Besides somatic cells, germinative cells also need to be able to have their DNA stable, to pass down the information to its descendants without errors or liabilities. However, the DNA is prone to damage, which can compromise its stability, consequently having an impact on the organism itself. Even though DNA mutations are an essential process that leads to evolution, the accumulation and the severeness of alterations in the genetic information can also result in extreme consequences for the cells' malfunction.

The damage inflicted upon the DNA can have different sources. It can be caused for example by environmental agents, mainly ionizing radiation or chemical agents [3]. When these factors interact with cells they can lead to DNA mutations, by directly disturbing the molecule bonds. Additionally, these factors can interact with the double-strand, distorting its structure in a way that can interfere with different processes like replication, transcription, or DNA repair. Environmental factors and endogenous metabolism can also affect DNA stability indirectly by the production of Reactive Oxygen Species (ROS) [4]. These are molecules that are prone to reacting with other structures, being able to target the DNA double-strand in several ways that will result in the loss of genetic stability. The ROS can for example oxidize the DNA, which will alter the DNA bases, or it can interact with the backbone as well. They can also promote the cross-link between the DNA and proteins, which will again interfere with DNA processes. Mechanisms such as replication and transcription can also cause DNA instability. When both processes intersect, they can cause a collision between the RNA polymerase II and the replication fork. This collision can lead to a Replication Fork Pause (RFP), making the strand susceptible to DNA damage and mutations [5, 6].

Necessarily, the cells have developed ways of repairing errors caused by DNA instability. For example, small DNA lesions, which are mainly caused by oxidation, such as mismatched bases, Apurinic/apyrimidinic (AP) sites, deaminations, or even Single Strand Break (SSB)s, can be repaired by Base Excision Repair (BER) [7]. DNA can also get wider and bulkier lesions, like Cyclobutane Pyrimidine Dimers (CPDs) or 6-4 photoproducts (two types of pyrimidine dimers caused by UV radiation), and other intrastrand crosslinks, between others. These can be resolved by Nucleotide Excision Repair (NER) mechanisms. DNA replication can also lead to errors such as mismatched base pairs and indels, which are small insertions and deletions in the strand. For these, the cell resorts to DNA Mismatch Repair (MMR). Other types of errors can also appear, like SSBs and Double Strand Break (DSB)s.

However, DNA Damage Response (DDR) not only resorts to repairing the DNA damage, but also includes mechanisms to preserve and prevent those lesions. Cell-cycle arrest, transcription regulation, telomere maintenance, and activation of the immune system are a few other processes where the DDR is involved [7]. Additionally, if the lesions are too severe to be repaired, DDR can also resort to cell death by regulating mechanisms like apoptosis [8].

Even though cells do have mechanisms that can repair or eliminate errors, this balance can be broken and the damage can accumulate and oversee the repairing, starting to have a detrimental effect on the cell and later the organism [9]. Therefore, DNA damage is known to be correlated with the induction of many diseases as well as the activation of tumorigenic mechanisms or even premature aging [10].

1.1.1 Double-Strand Breaks

Genome instability can lead to the occurrence of SSBs or DSBs, being the second one of the most severe consequences of damage in the DNA. As the name suggests, in this type of lesion both strands of the helix break in the same base pair, resulting in the separation of the two newly formed strands.

The DSBs can be induced by different methods. As referred in Section 1.1, DSBs can be induced not only by ionizing radiation (X-ray or gamma rays) or non-ionizing radiation (laser microirradiation) but also by chemical agents [11]. Chemicals like camptothecin can inhibit topoisomerases, which are enzymes that catalyze changes in the topological state of DNA. Their inhibition has been shown to lead to the formation of DSBs. Forming these lesions by replication fork collision is also possible. Artificially, by using replication inhibitors such as Hydroxyurea (HU) or aphidicolin, or crosslinker agents, like cisplatin or mitomycin C can also be used to form replication fork collapses, thus inducing the DSBs [11]. However, to induce breaks by directly targeting the DNA strand, molecules like the Neocarzinostatin (NCS) are used. This agent, which is part of the chromoprotein antitumor antibiotics family, was first isolated from *Streptomyces carzinostaticus*, a type of bacteria [12]. It is known that NCS can induce DSBs *in vitro* as well as *in vivo*, and its

mechanism of action is well known: The NCS possesses a chromophore in its structure that is the one responsible for its biological relevance. It binds to the DNA double-strand in a non-covalent way, having a preference for minor grooves. When there are available thiol molecules in proximity, the NCS chromophore forms a highly reactive bi-radical species and proceeds to interpolate between adjacent DNA base pairs. This results in an alteration and destabilization of the DNA strand, thus making it break [13].

1.1.2 DNA Damage Response of DSBs

As previously stated in Chapter 1.1, DSBs are one of the lesions that can be repaired by DDR. It can be repaired mainly by two processes: Non-Homologous End Joining (NHEJ) and Homologous Recombination (HR). In both mechanisms, the recognition of the DSB is made by the Mre11-Rad50-Nbs1 (MRN) complex, which will bind to the strand ends and recruit other factors, such as kinase Ataxia Telangectasia Mutated (ATM) and Ataxia Telangiectasia and Rad3 related (ATR) [14, 15] (Figure 1.1). This protein is capable of phosphorylating histone H2AX, thus decondensing the chromatin, allowing the recruitment of DNA repair factors and checkpoint proteins [16]. Depending on the balance between the factors recruited, different DDR are initiated [17].

For the NHEJ it is usually required the recruiting of the 53-Biding Protein 1 (53BP1), which binds to the H2AX and promotes the DNA repair (Figure 1.1). The pathway then proceeds with the binding of Ku proteins (a dimeric protein complex) to the break site, which will allow the recruitment in a cascade of various factors [18, 19]. Between them is included the recruitment of DNA-dependent Protein Kinase catalytic subunits (DNA-PKcs) [20], member of Phosphatidylinositol 3-Kinase-related Kinase (PIKK) family, and also the recruitment of X-ray Repair Cross-Complementing protein (XRCC4) [18]. These will bind to the DNA-Ku complex, which will further stabilize the structure. Consequently, the remaining factors, mainly constituted by enzymes (e.g., Artemis, Werner (WRN), and Aprataxin-and-PNK-like Factor (APLF); [21–23]), will help with the processing of the strand ends, which implies resection of the DNA ends, filling the gaps, and removing blocking end groups. Finally, the XRCC4 also promotes the recruiting and activation of DNA Ligase IV, thus allowing the ligation of both ends [24].

In HR, after the recognition and binding of the MRN complex, there is a recruitment of the Exonuclease 1 (Exo1) [25] and SUMO-activating Enzyme subunit 2 (SAE2) protein [26], that will participate in the 5'-end resection. After this, there is the formation of 3' overhanging tails in both strands. On these single-strand ends will then bind and form Replication Protein A (RPA) filaments, that temporally inhibit the biding of Rad51 filaments, but at the same time stabilize and prevent the biding of other unwanted factors in the strands [27] (Figure 1.1). However, the biding of Rad51 proteins starts to overcome the RPA's affinity with the help of mediators, such as Breast Cancer Type 1 (BRCA1) and Breast Cancer Type 2 (BRCA2) proteins [28, 29]. Consequently, there is a formation of Rad51 filaments in the 3' overhanging tails, which will allow the initiation of the strand

invasion into a template DNA. This template strand will be used as a reference to correct the damaged strand ends.

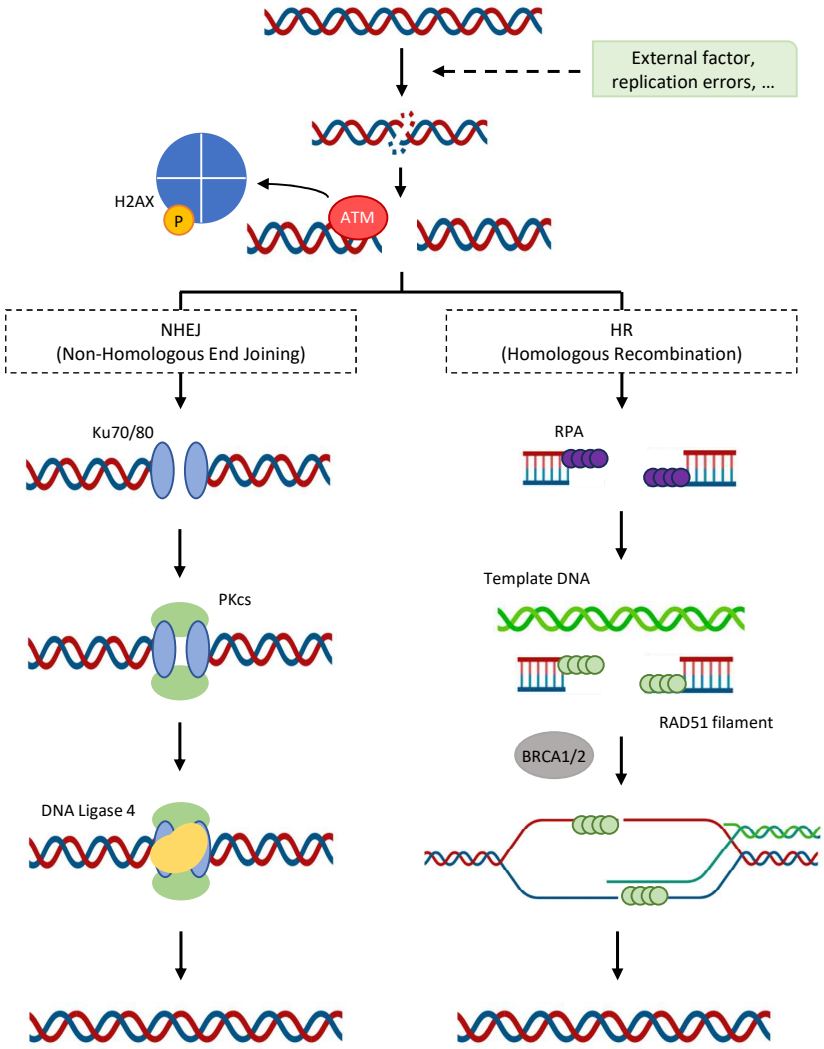

Figure 1.1: Scheme of DSB induction and possible DDR mechanisms in cells. The DNA can be damaged by various agents (e.g. chemical agents, replication errors, ...), and that can lead to the formation of DSBs. However, these can be repaired by the cell in a process that starts with the recognition of DSBs by ATM. This molecule will then phosphorylate the histone H2AX, which enables the recruitment of DDR factors and the repair initiation. One of the two most common mechanisms utilized by the cell is the NHEJ. In this one, Ku70/80 proteins bind to the DSB ends and recruit PKCs, thus stabilizing the cell and recruiting other factors such as the DNA ligase 4, that will repair the strand. The other most common mechanism is the HR, which starts with the binding of RPA in the 3' extended ends. With the help of other proteins such as BRCA1 and BRCA2, there is RAD51 filaments formation, thus allowing strands to exchange between the damaged DNA and the sister chromatid. This will function as a template for the damaged DNA, which will then be repaired.

In general, the NHEJ is a mechanism that can repair the DSB by stabilizing and ligating both ends without any template. This, together with the fact that NHEJ is cycle independent, is faster than HR, and also suppresses in some cases HR mechanism, makes this pathway the one preferred and used for the repair of the majority of DSBs [30–32]. However, NHEJ is also really prone to errors and leads to unwanted chromosomal

rearrangements in one-ended DSB, that can occur during replication fork collapses [33]. On the other hand, the HR is used less regularly and on more specific occasions but usually does not lead to as many errors as the other repair mechanism. One reason for that is that the HR uses a template DNA, usually a sister chromatid, which leads to a more accurate repair [34]. However, because this technique needs a template, it is cell cycle-dependent, meaning that the cell needs to be at the S or G2 phases of the cell cycle since it is when there is enough genetic material to proceed [35]. Some studies show that HR can occur outside of those phases (e.g. G1 phase), but usually just happens in specific cases and it uses repetitive sequences as a template to repair the DSB [36, 37]. To repair DSBs there are also alternative pathways, such as Alternative End-joining (a-EJ) [38]. This repair mechanism is similar to NHEJ, but it uses small homologous sequences of both ends to catalyze its ligation. Consequently, a-EJ is an error-prone technique, since it results in small deletions near the break, to form microhomologous ends.

Even though the repair of DNA damage is crucial for the organism's good function, the lack of efficiency of these pathways in aging and in diseases is well established, especially in tissues like muscle fibers. Therefore, despite not existing much research on these repair mechanisms in post-mitotic cells like the skeletal muscle, it is important to better understand their relation so that it is known how these cells deal with DNA damage and recover their efficiency.

1.2 Skeletal muscle

The skeletal muscle is a specific type of muscle tissue present in some organisms, mostly in vertebrates. It is responsible not only for the production of contractile forces, which allow body movement but also for stabilizing the skeleton and body posture. It is also responsible for other functions, such as involuntary movement (like breathing or swallowing) or body temperature regulation [39]. The skeletal muscle is composed mainly of organized bundles of muscle tissue, blood vessels, and nerves, which are all surrounded by connective tissue sheets (forming the epimysium) (Figure 1.2). This tissue complex will then connect to the bone's tendons, to transmit the force generated by the fibers into it. Each bundle of muscle tissue is composed of myofibers, which are composed of blood vessels, nerves, and majorly myofibrils, and surrounded also by connective tissue (endomysium). Myofibrils are elongated muscle cells and in each one of these, there is the formation of structural units called sarcomeres. These units are composed of protein filaments, the most important being myosin and actin, which can interact with each other, thus generating the contractile forces responsible for the muscle function [40, 41].

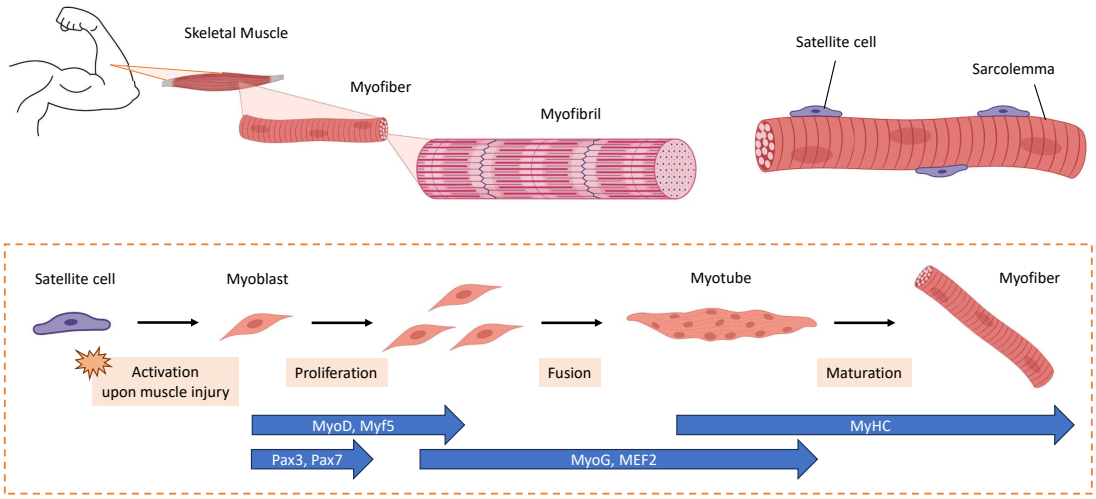

Figure 1.2: Skeletal muscle physiology and satellite cells differentiation scheme. Vaguely, the skeletal muscle is composed of many myofiber clusters, each myofiber being composed of many myofibrils (structures responsible for muscle contraction). Each myofiber is an elongated and multinucleated specialized muscle cell, that forms during the development of the muscle. The process starts with the activation of the proliferation of MyoB (myofiber precursors) by the expression of transcription factors such as Pax3 and Pax7 and others that also appear during earlier stages of fusion (e.g. MyoD and Myf5) when the MyoB start to fuse. This process is mainly controlled by the expression of proteins like myogenin and MEF2. There is also maturation which is usually detected expression of MyHC protein. During muscle injury in the muscle, there is activation of satellite cells (nondifferentiated cells localized next to the sarcolemma membrane in developed myofiber) that will also differentiate and fuse with the damaged myofiber, regenerating it.

1.2.1 Muscle cells differentiation

During embryonic development, the muscle progenitor cells are firstly regulated by the transcription factor Paired-box protein 3 (Pax3) (or the orthologue protein Paired-box protein 7 (Pax7) for adult skeletal muscle differentiation) that will control their migration from the somites, more specifically, the dermomyotome [42]. Once these cells, now denominated Myoblasts (MyoB), reach the limbs, they start to proliferate. In the final step of this stage, there is expression of proteins like Myf5 and MyoD [42, 43], which are Myogenic Regulatory Factors (MRF) of muscle-specific genes, which will be essential to muscle differentiation. However, it was shown that they might also help with the cell's proliferation since they also appear in smaller quantities during this time [44]. Small expression levels of Pax3 are still present at the beginning of the proliferation stage, suggesting that this protein might help retain the proliferation. The expression of proteins like myogenin and MEF2 will then lead to the differentiation of the MyoB [45]. This process consists of the fusion between these cells, resulting in the fusion of their nuclei and formation of Myotubes (MyoT) and later their maturation into fully developed myofibers [46] (Figure 1.2). Because of this process, the MyoT/myofibers become cells that are elongated and multinucleated, meaning that they possess many nuclei in each cell, a rare but not unique trait in the human body (hepatocytes and osteoclasts share this characteristic as well).

Besides not directly influencing cell differentiation, other proteins have been shown

to follow their expression level according to myofiber formation. One of those is the desmin protein, which is an intermediate filament that stabilizes the structure of the sarcomeres. This protein shows to increase its expression during cell proliferation until cell differentiation [47]. Another protein that presents similar levels of expression is the dysferlin protein, a membrane protein found in the sarcolemma, that aids in the repair of this membrane when it gets damaged [48]. We also have the example of the Myosin Heavy Chain (MyHC) protein, which is a motor protein responsible for the induction of contractile forces in the sarcolemma structures. Opposite of the other two examples that express through the all process, this protein gets only expressed in later stages of muscle differentiation [49].

In Table 1.1 are represented the differentiation markers mentioned above and the respective expression patterns during skeletal muscle differentiation at different stages.

Table 1.1: Expression of different proteins during muscle cell differentiation. List of different proteins involved in MyoB differentiation (Pax3, Pax7, MyoD, Myf5, and myogenin) or proteins present in the muscle composition (MyHC, desmin and dysferlin). It shows their respective expression during adult stem cells/satellite cells activation, MyoB proliferation, and MyoT/myofibers differentiation. All these proteins have been shown to work as biomarkers for muscle cell differentiation.

Marker	Satellite cell Activation	MyoB Proliferation	MyoT Differentiation
Pax3	-/+	-	-
Pax7	+	-	-
MyoD	-	++	+
Myf5	-/+	+	-
Myogenin	-	-	+
MyHC	-	-/+	+
Desmin	+	+	++
Dysferlin	+	+	++

1.2.2 Local injury in muscle cells and satellite cell differentiation

Myofibers are post-mitotic cells, meaning that they stop proliferating after being terminally differentiated. At the same time, the muscle tissue can be injured as a consequence of some external factor or ruptured due to mechanical stress caused by muscle contraction. And so, this can lead to the compromise of the myofiber integrity, thus damaging the cells that cannot be replaced by new ones. However, at the same time, the muscle cells also show impressive repairing capacity, being able to fully regenerate after a short period upon damage [50]. The reason for this is that the muscle cells utilize differentiation to renew the nuclei of injured myofibers. This is possible because there are cells that emerge from the same origin as embryonic muscle progenitors in fully developed muscle fibers [51]. These cells are called satellite cells and they retain their nonspecific form in an inactivated state (quiescent cells). These types of cells can be found in the muscle fiber, in an asymmetric niche between the sarcolemma (muscle plasma membrane) and the

basal lamina, that surrounds the periphery of myofibers. Therefore, these cells can be activated and recruited by the injured myofiber, where they start to proliferate and fuse to it, adding more nuclei to the cell, thus repairing the damage dealt [52]. Afterward, the cells reactivate their quiescent state, to replenish the niche of satellite cells [53]. However, the efficiency and the amount of satellite cells are greatly influenced by variables such as injury severity, age, organism, muscle type, and location [54].

What triggers the satellite cells activation, which signals the myofibers secrete to activate them, and how the communication between these cells work, are still questions that need to be more elucidated to be fully understood.

As referred before, muscle injury is able to activate satellite cells. The reason for that is the disruption of the basal lamina, which works as a protective membrane for the satellite cells niche. Damaging this membrane can lead to the detachment of the satellite cells, which has been shown to contribute to their activation [55]. Additionally, the satellite cells' niche environment seems also to play an important role in muscle repair efficiency. Muscle tissues of aged mice were able to restore some of their genetic expression by adding young mice satellite cells' niche [56, 57]. However, damaging the fibers without perturbing the membrane also leads to satellite cell activation [58], confirming that there must be communication between the two types of cells. Muscle injury can also inflict damage on other types of tissues such as blood vessels and Extracellular Matrix (ECM), that will contribute to the satellite cell activation, by the secretion of agents like Hepatocyte Growth Factor (HGF) [59, 60]. Additionally, muscle injury can also trigger the invasion of immune cells or inflammation, which will also lead to immune cells recruitment. This immune cell infiltration has also been shown to activate satellite cells [61, 62]. Therefore, these findings also established a relationship between muscle regeneration and immune response, which could be important for understanding the role of DNA damage in muscle regeneration. This is due to the fact that DNA damage is closely related to ROS production, as it will be explained later, and ROS can contribute to inflammation.

As for the agents that can play a role in the activation of satellite cells, it has been shown that MyoB differentiation can be activated during exercise by secretion of molecules like 8-oxoG base, by activation of the Ras-MEK-MyoD pathway [63]. Additionally, Platelet Derived Growth Factor subunit B (PDGF-B) secretion in muscle cells seems to increase during MyoB differentiation and enhances MyoB proliferation as well as MyoT maturation [64]. There are also reports of secretion of Nitric Oxide (NO) and HGF, in a NO-dependent manner, during muscle injury, that show to activate the satellite cells by binding to the c-met receptor of these same cells [59, 65, 66]. Not only those, but other molecules, especially growth factor (e.g. Insulin-like Growth Factor 1 (IGF-1) [67], Fibroblast Growth Factor 6 (FGF6) [68], or even Transforming Growth Factor-beta (TGF-b) [69] in specific cases), have also been shown to play a role in activating satellite cells upon muscle injury.

Secretion pathways of injured MyoT have still not been very explored. However, it is known that MyoB, while differentiating, are able to secrete exosomes (Figure 1.3). These usually have in them RNA material that has been shown to interact with muscle cell

proliferation/differentiation factors, such as Pax7 [70] and sirtuin-1 [71]. It was also proven that these exosomes not only interact with MyoB but also promote myofiber regeneration by activation of satellite cells [72, 73]. Besides exosomes, there is also secretion of microvesicles through membrane blebbing and protein soluble secretion by conventional secretory mechanisms in differentiating MyoB [73] (Figure 1.3). These possess conventional and non-conventional signal proteins for myogenesis that might interact and activate satellite cells for muscle regeneration.

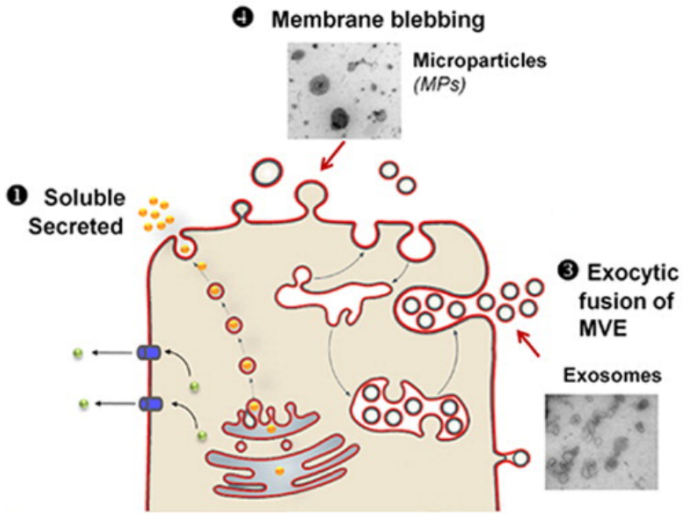

Figure 1.3: Types of secretion in differentiating muscle cells. Representation of different types of secretion encountered in MyoB during differentiation. Firstly, factors can be secreted by conventional secretory mechanisms, for example by using the Endoplasmic Reticulum (ER)-Golgi pathway. Factors can also be secreted inside vesicles, such as microparticles or exosomes. Adapted from *Le Bihan, Marie-Catherine et al. "In-depth analysis of the secretome identifies three major independent secretory pathways in differentiating human myoblasts." Journal of proteomics vol. 77 (2012)* [73]

Lesions in the skeletal muscle can cause rupture of the muscle tissue but can also induce DNA damage in the cells [74]. Moreover, the muscle's own metabolism can lead to the production of ROS that can lead to DNA damage as well [75], as referred in Chapter 1.1. Therefore, besides knowing how injury affects muscle fibers, it is also important to better understand how the muscle responds to DNA damage.

1.3 DNA damage in muscle cells

As shown earlier, it is known how the skeletal muscle repairs its cells after being mechanically injured. However, there is still little evidence on what type of DDR muscle uses upon having their DNA severely damaged. Furthermore, even though DDR mechanisms are well established in proliferating cells, studies in post-mitotic cells, such as muscle fibers, are still really poor.

It has been shown that DNA repair is attenuated in damaged post-mitotic cells and that the capacity of repairing expressed genes is still maintained [76]. Differentiated muscle cells also show a lack of BER, which is the main mechanism to resolve small base

lesions like previously stated [77]. On the other hand, there is evidence that NER, which repairs bulk DNA lesions, is still preserved. The NER mechanism can be divided into sub-pathways, one of them being the Transcription-Coupled Repair (TCR), which is the one believed to be responsible for the expressed genes efficient repair [76, 78].

Myofibers are post-mitotic cells, therefore the HR mechanism cannot be used as DDR pathway in these cells. Since this pathway is cell cycle-dependent (available normally only during S and G2 phases) it seems unfit that the muscle cells use HR because they cannot undergo mitosis. In fact, unpublished data from the host group confirmed that MyoT indeed does not utilize HR while dealing with DNA damage. Logically, NHEJ would be suited as a good candidate to be used by the cells since it is cell cycle independent. However, the same unpublished data showed longer DDR response in MyoT when compared to MyoB, which is contradictory, since NHEJ is in general a faster process than HR. Moreover, the accumulation of error due to the use of NHEJ would probably put too much pressure on the cell's survival. Additionally, although the mechanisms for DDR in the muscle cell are deprived, these cells possess mechanisms that prevent cellular death. Indeed, a study showed that myofibers show a lack of p53 protein expression, a transcription factor involved in the apoptosis pathway [79]. Consequently, myofibers are one of the longest-living cells in our body, thus revoking the possibility of cell death as a response to DNA damage.

On the other hand, the lack of renewal of differentiated muscle cells also makes them susceptible to the accumulation of errors. Together with the fact that regenerative efficiency decreases with aging, myofibers can induce many diseases that are related to DNA damage.

1.3.1 Muscle diseases involved with DNA damage

Many myopathic disorders in skeletal muscles have been associated with damage to the DNA. Duchenne Muscular Dystrophy (DMD) and Limb Girdle Muscular Dystrophies (LGMD) are two diseases with no cure that can be categorized by progressive muscle weakness and degeneration, due to the mutation of genes like dystrophin and dysferlin (for type 2B) respectively. Patients with DMD and LGMD type 2B present an accumulation of DNA damage in the muscle tissue. Not only that, but this increase also appears in early MyoB cell cultures as well as in DMD fetuses and young patients, suggesting that the damage occurs during the early stages of the disease and might work as a cause rather than a consequence [80]. In patients with Emery–Dreifuss Muscular Dystrophy (EDMD), which is also a muscular dystrophy characterized by muscle weakness and joint contractures, there is disruption of the DNA repair machinery. This is due to alterations in proteins of the nuclear lamina, such as Lamin A/C, that has been linked to DDR, or Nuclear envelope transmembrane protein 39 (Net39), that disrupt the genome stability and promote premature aging [81, 82]. In fact, many other laminopathies have been correlated with DDR deficiency. One of those cases is the Hutchinson–Gilford progeria syndrome

which is a disease characterized by accelerated aging in early childhood. This disorder is caused by mutations in the *LMNA* gene, which have shown higher DNA damage levels prior to the onset of the dystrophy [83]. Facio-Scapulohumeral Dystrophy (FSHD) is also a disease that develops muscle atrophy. Patients who suffer from this condition show myofibers that are more susceptible to oxidative stress, accumulating more DNA damage. This is due to *DUX4* expression, a transcription factor expressed during early embryonic development and silenced in adult tissues, and morphological defects in the MyoT [84, 85]. The majority of muscular dystrophy sarcomas also show an increased occurrence of DNA damage, more specifically, higher DSB levels. In mice, these lesions appear before the sarcoma, suggesting once more that DNA damage is the cause of the disease [80].

The treatment for these diseases is rather complicated since it affects the MyoT regeneration capacity. The MyoT need to be injured or get its DNA damaged to activate satellite cells and regenerate. However, at the same time damaging the cells and their genetic information also damages the myofibers and leads to disease formation. It can also damage satellite cells, which inhibits them from proliferating and differentiating. Because the majority of DNA damage comes from ROS formation, antioxidants have shown progress in satellite cells proliferation as well as MyoT formation, regeneration, and better function [86–88]. However, too many antioxidant treatments lead to differentiation inhibition [88].

Therefore the majority of these diseases still do not have a treatment, magnifying the importance of studying the effects that DNA damage has on the muscle cells and the repair mechanisms behind it. However, as referred in Chapter 1.3, there is a lack of DDR mechanisms and a blockage of cell death pathways in these cells. Altogether, this data suggests that myofibers use a novel mechanism to repair DSBs. Strikingly, results followed by the same unpublished data from the host group greatly suggests that autophagy is involved in the DDR for these type of cells. More specifically, there is evidence that the myofiber uses autophagy in DNA that was damaged (nuclear autophagy) to remove it from the nucleus and probably degrade it or remove it from the cell.

1.3.2 Autophagy

The mechanism by which the cells eliminate intracellular components is called autophagy. This mechanism is a highly conserved degradation process in cells that plays a crucial role in the cell homeostasis. It is involved in cell differentiation as well as in the organism longevity [89] and disease formation [90]. This mechanism is initiated by the formation of phagophores, which are double-membrane structures that are highly regulated by nutrient sensors proteins like Mammalian target of rapamycin (mTOR) [91], AMP-activated Kinase (AMPK) [92] and the Phosphatidylinositol 3-kinase Class III (PI3KC3) complex (produces Phosphatidylinositol 3-phosphate (PI3P), that helps with the vesicle nucleation in the cytoplasm, [93]). The phagophores will then elongate, which is also a mechanism regulated by PI3P, that recruits other autophagy factors and regulates endocytic membrane trafficking [94]. Other proteins also play a role in autophagosome maturation such as

Microtubule-associated protein 1A/1B-Light Chain 3 (LC3), which phosphorylates during autophagy and helps with membrane stability [95], or the Autophagy-related (ATG) proteins family, that, as the name suggests, have many functions through all autophagy process [96]. The phagophore proceeds to close, forming a double-layer vesicle, the autophagosome. This vesicle will then fuse with a lysosome with the help of docking and membrane fusion proteins (e.g., Snap Receptor (SNARE) complex) [96]. Consequently, the vesicle material will be degraded inside the complex by the action of various enzymes.

1.3.3 Nuclear autophagy

The majority of studies related to autophagy are directed to the degradation of cellular molecules in the cytoplasm. However, it is also possible to degrade nuclear material (selective nuclear autophagy, simply known as nucleophagy) and even in specific cases, the degradation of the whole nucleus. It was first observed in yeast [97], however, it can be also found in a few eukaryotes, such as *Tetrahymena thermophila*, which is a unicellular organism that at a point in time, after germination, has two nuclei and eliminates its parental nucleus by nuclear autophagy [98]. We also have the example of the fungus *Aspergillus oryzae*, which besides using autophagy, is also a multinucleated organism that eliminates specific nuclei under stressed conditions [99]. Even in mammals, it can be observed autophagy that includes degradation of nuclear vesicles [95], however, there are no reports of autophagy of DNA material nor the elimination of the whole nucleus.

Nuclear autophagy can be divided into different types and different organisms can show different types respectively. The most common is the macronucleophagy, which is also the one encountered in mammals. In this mechanism, the double-membrane vesicle is formed using the nuclear membrane, probably in a similar method used in exocytosis. Since LC3B-II (an active form of LC3B) exists inside the nucleus, this might interact with Lamin-B1, which is a protein located in the inner nuclear membrane that participates mainly in the nuclear structural support. Thus the interaction between the two might allow the vesicle formation. The vesicle will then fuse in the lysosome in the cytoplasm and degrade the nuclear material [95]. Another type of autophagy that can be observed in mammals is the micronuclear autophagy. In this technique, there are extranuclear bodies, known as micronuclei, that have inside chromosomal fragments derived from poor chromosome segregation during cell division. These have been proven capable of fusing to lysosomes and have their components degraded [100].

If the muscle cells are relying on nuclear autophagy to eliminate the damaged DNA, it means that the cells are constantly losing genetic information over time. The severe loss of genetic information would be critical for the muscle cells, which would be deteriorating at rapid progression. One way of compensating for this loss of information would be activating the satellite cells, which would then help with muscle regeneration.

1.4 Project Aims

The muscle cells are post-mitotic cells, which means that their regenerative methods are deprived. At the same time myofibers, when compared to their precursors, do not resort to cell death as a way to respond to damage. This suggests that the muscle cells have an alternative way of dealing with damaged genetic information, or else the cells would be accumulating errors over time, which would be harmful to the cells. There is strong evidence that shows that the muscle cells use nuclear autophagy to eliminate the damaged DNA. However, that would also lead to the progressive loss of DNA damage, therefore, the muscle cells have to compensate for that loss somehow. Since muscle cells are also multinucleated cells, our hypothesis is that they are activating satellite cells the same way that it happens during muscle mechanical injury. In this project, we are suggesting that, after the DNA of muscle fibers gets damaged and eliminated by nuclear autophagy, it is triggered secretion of agents, in a mechanism in which we denominated DNA Damage-Associated Secretory Phenotype (DASP). These agents would be able to activate the satellite cells, which would later proliferate and differentiate, thus fusing to the damaged myofiber. The genetic loss of that cell would be compensated with the new DNA of the satellite cell nuclei (Figure 1.4).

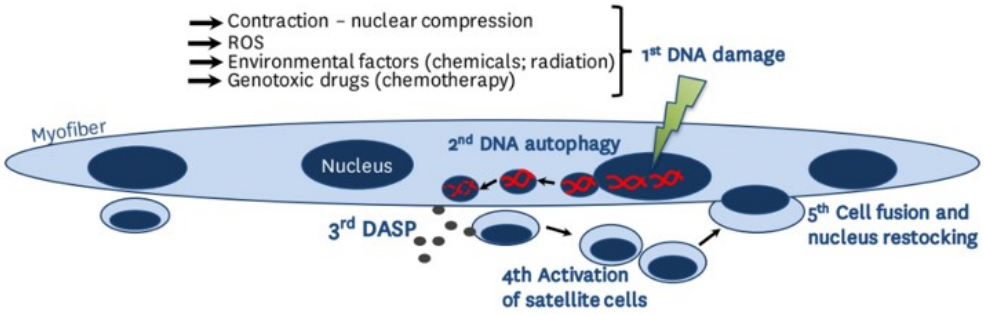

Figure 1.4: Proposed model of DDR in skeletal muscle cells. The myofiber is a multinucleated cell and a certain nucleus can get its DNA damaged by various factors. Consequently, the damaged DNA is recognised and it occurs nuclear autophagy (mechanism unknown) that will remove and degrade the DNA. There is then a secretion of agents (DASP) that will activate nearby satellite cells, thus recruiting them to the respective myofiber (by an unknown mechanism). The loss DNA will be replaced by the fusion of the activated satellite cell and the integration of its nuclei.

To study the way that muscle fibers respond to DNA damage, this work was divided into 3 main objectives.

The first objective will be to solidify the evidence provided by the unpublished data from the host group that nuclear autophagy is involved in DDR of muscle cells. We hypothesize that the nuclei of damaged Myot have nuclear protrusions or vesicles that would indicate the formation of autophagosomes. To do that, it will be needed to analyze the nuclei of these cells by Electron Microscopy (EM) and compare them with normal MyoT nuclei.

The second objective revolves around identifying the composition of the secretome of damaged myofibers. As referred earlier, we suggest that after the elimination of the

damaged DNA, there is a DASP mechanism in which are secreted agents that activate satellite cells. Therefore, we will analyze the composition of the conditioned medium of DNA damaged MyoT by Ultra Performance Liquid Chromatography–Mass Spectrometry (UPLC-MS) and compare the significant metabolites with state-of-the-art molecules that already are known to be related to the regeneration of muscle injury.

For the final objective, we will confirm the activation of satellite cells by DNA-damaged myofibers. The constant loss of genetic information due to nuclear autophagy leads us to believe that satellite cells are activated to replenish the DNA of damaged muscle cells. In order to confirm this hypothesis, we will damage MyoT, collect their conditioned medium, and treat MyoB with the respective secretome to see if these cells differentiate. The analysis of the MyoB will be done by using different techniques, such as Western Blot (WB), Reverse Transcriptase quantitative Polymerase Chain Reaction (RT-qPCR), and Immunofluorescence (IF), against several differentiation biomarkers: desmin, dysferlin, myogenin, MyHC or Myosin Heavy Chain 3 (MyH3) (an isoform of MyHC), and MyoD proteins.

2

Materials and Methods

2.1 MyoB and MyoT cell culture

In this project, we used Human Skeletal Myoblasts, KM155 cell line, established by Vicent Mouly from the Institut de Myologie UPMC Université Paris France [101]. The cells were grown in Skeletal Muscle Cell Growth Medium (PromoCell C-23060) supplemented with a mix containing Fetal Calf Serum (0,05 mL/mL), Fetuin (50 μg/mL), Epidermal Growth Factor (10 ng/mL), Basic Fibroblast Growth Factor (1 ng/mL), Insulin (10 μg/mL) and Dexamethasone (0,4 μg/mL). Once the MyoB reached an 80-90% confluency the medium was removed and washed with Phosphate-buffered Saline (PBS) 1x, to initiate cell differentiation through serum starvation. For that, we added differentiation medium to the cells. The differentiation medium is composed of Iscove's Modified Dulbecco's Medium (IMDM GlutaMAX™ Supplement – Alfagene 31980022) and Ham's F-10 Nutrient Mixture (F-10) (Alfagene 41550021) with a ratio of 1:1 supplemented with 1% ITS (I1884 Sigma Aldrich - Contains 1.0 mg/mL recombinant human insulin, 0.55 mg/mL human transferrin (substantially iron-free), and 0.5 μg/mL sodium selenite at the 100x concentration). The cells were differentiating for 5 days and the medium was renewed on the third day. A generalized experimental setting scheme is shown in the Supplementary Figure I.1. All cells were maintained at 37°C in a humidified atmosphere containing 5% CO_2.

In the experiments performed to analyze MyoT differentiation over time, MyoB were cultured into gridded glass bottom dishes (81166 - iBidi - μ-Dish 35 mm, high Grid-500 ibiTreat). The plates were coated with Matrigel (Corning® Matrigel® Growth Factor Reduced (GFR) Basement Membrane Matrix, *LDEV-Free, 354230) at a dilution of 1:100 for 1 h at 37ºC. The plates were then washed twice with PBS 1x before adding the cells. The cells were analyzed/collected on each day of differentiation (day 0 to day 5). For the remaining experiments, cells were cultured in 6-well plates.

2.2 DNA damage induction and conditioned medium preparation

To induce DNA damage, we treated MyoT with 0.5 μL of 2.5 μM of NCS for 30 min on the fifth day of differentiation. After that period of time, the medium was washed with 1 mL of PBS 1x, and Skeletal Muscle Cell medium was added.

To prepare the Conditioned Medium (CM) samples, half the wells containing MyoT were incubated with NCS as previously explained. The CM was then collected at different time points and added to MyoB culture at a confluency of around 50-60%. While in some samples the conditioned medium was just added on the first day (No Renewed (NR)), in other samples the medium was replaced every day during differentiation (Always Renewed (AR)). As controls, it was also prepared a condition of just MyoB and another with fully differentiated MyoT. For some experiments, a different experimental setting was made. After having MyoT fully differentiated, two samples were treated with NCS. However, one of them was also incubated with 1 μL of 2.5 μM of Ataxia Telangectasia Mutated inhibitor (ATMi) (KU55933, Enzo Life Science) before and after the incubation with NCS. The respective CMs were moved to another 6-well plate with MyoB with a confluency of 90%. In that plate were also prepared MyoB and MyoT conditions as the controls and MyoB incubated with NCS. A generalized experimental setting scheme is shown in the Supplementary Figure I.1.

2.3 Fusion Index

The Fusion Index (FI) was calculated by counting the number of nuclei in MyoT (cells with 3 or more nuclei in the same cell) relative to the total number of nuclei counted, in percentage. The images were acquired using Zeiss LSM 880 confocal point-scanning microscope (Carl Zeiss) and the ZEN Microscopy Software (Carl Zeiss).

For the MyoT differentiation through the days, approximately 300 to 500 nuclei were counted, while in the MyoB treated with the CM, around 700 nuclei were counted.

2.4 Western Blot

Western Blot (WB) is a technique that can separate proteins based on their molecular weight. It is primarily a qualitative method that can detect the presence of protein expression but also has some semi-quantitative capacities by enabling the comparison of specific protein expression through analysis when performed in specific conditions.

To collect the samples for the WB, the cells were washed with PBS 1x and lysed with Laemmli Buffer 2x (80 mM pH 6.8, 16% glycerol, 4.5% Sodium Dodecyl Sulfate (SDS), 450 mM Dithiothreitol (DTT), 0.01% bromophenol blue and water, supplemented with 100 U benzonase (Sigma Aldrich) and 1% (v/v) $MgCl_2$) using a scrapper in the plate's wells. The lysate was incubated for 20 min at Room Temperature (RT) and the samples

were stored at 4ºC. The samples were then boiled at 100ºC for 5 min and centrifuged for 2 min at 14.1 xg to remove any impurity or nucleic acids still bound to the proteins. The samples were loaded to a polyacrylamide gel (4.5% stacking gel and 6 or 12% running gel, their composition is in the Supplementary Table I.6 and I.3) by pipetting 8 μL of each condition together with 8 μL of a mixture of 1:1 color protein marker (MB09002, NZYTech) with Laemmli Buffer 2x. The gel was resolved by SDS-Polyacrylamide Gel Electrophoresis (SDS-PAGE) in a Mini-PROTEAN Tetra Vertical Electrophoresis Cell (Biorad) chamber, with a voltage of 15 mA per gel.

The gel transfer to a nitrocellulose membrane was performed using a semi-dry transfer system (Invitrogen™ iBlot™ 2 Gel Transfer Device (Fisher Scientific) and Invitrogen™ iBlot™ 3 Transfer Stacks (Fisher Scientific)). The transfer process was conducted at 20 V for 7 min. The membrane was then incubated with Ponceau Red 1% in dH_2O to be able to see the bands and confirm the efficiency of the transfer, and washed with PBS 1x containing 0,05% (v/v) Tween 20 (PBS-Tween).

Afterward, the membrane was blocked by incubating with 5% (m/v) milk in PBS-Tween for 1 h, at RT. Then the membrane was incubated with the primary antibodies with a 1:1000 dilution in 5% (m/v) milk in PBS-Tween at 4ºC, overnight (o/n). The following antibodies were used in this study: rabbit anti-Dysferlin (Abcam, ab124684), mouse anti-MyHC (Developmental Studies Hybridoma Bank, MF20), mouse anti-Desmin (Dako, D3), Histone H3 total (Abcam, ab1791), mouse anti-α-tubulin (Sigma, T5168), rabbit anti-Myogenin (Abcam, ab219998). The membrane is then washed 3 times, 5 min, with PBS-Tween and incubated with the respective secondary antibodies with a 1:5000 dilution in 5% (m/v) milk in PBS-Tween, 1 hour at RT. The membrane is once more washed 3 times, 5 min, with PBS-Tween. The detection of the proteins was done by a chemiluminescence method. In this reaction, it is used a secondary antibody conjugated with Horseradish Peroxidase (HRP). The membrane was soaked for 1 min with the enhanced chemiluminescent substrate luminol (ECL Western Blotting Detection Reagents (Cytiva) or Super Signal West Femto Maximum Sensitive Substrate (Thermo Scientific) for scarce proteins). The reaction between the enzyme and the substrate emits light at 428 nm, which was analyzed using an Amersham ImageQuant 800 GxP biomolecular imager (Cytiva). The images were taken every 15 seconds until reaching 30 recordings.

2.5 RNA isolation and quantitative RT-qPCR

The Polymerase Chain Reaction (PCR) method is a technique for amplifying a specific DNA or RNA chain. Firstly, there is denaturation, where the genetic material is heated, thus separating the DNA strands. Afterward, there is the annealing step, where small sequences called primers (small sequences that specifically target the DNA) bind to the complementary target. Finally, there is the extension of the strands, where the DNA polymerase uses the primers to catalyze the remaining complementary strand, reaching a high amount of copies of that sequence. For this work, it was used RT-qPCR, which

combines real-time or quantitative PCR (allows the measurement of RNA through time), and reverse transcription, where complementary DNA (cDNA) is used as a template for the reaction.

The entirety of the protocol was made on ice unless told otherwise. RNA isolation was performed as follows. First, the samples were washed with 1 mL of cold PBS 1x. Then it was added 500 μL of trypsin to the samples, which were incubated for 5 min, at 37ºC. Next, we added 1 mL of PBS 1x, and the samples were centrifuged at 1500 xg, for 5 min, at 4ºC. Afterwards, the supernatant was discarded and the samples were washed and centrifuged once more. The resulting pellet was resuspended in 1 mL of tryzol and incubated for 5 min at RT. Then, we added 200 μL of chloroform, and the samples were incubated for 3 min at RT, following another centrifugation at 12000 xg for 15 min at 4ºC. After centrifugation, the upper phase was transfered to another Eppendorf tube, in which we added 500 μL of isopropanol (2-propanol), incubated for 10 min at RT, and centrifuged at 12000 xg for 10 min at 4ºC. Subsequently, the supernatant was discarded and the pellet was washed with 1 mL of EtOH 75%, followed by a centrifugation of 7500 xg for 10 min at 4ºC. The supernatant was again discarded and the pellet, after dying, was resuspended in 23 μL of DNase/RNase-free water (Water for Molecular Biology, NZYTech). In a new Eppendorf tube was added 5 μg of RNA, 5 μL of Buffer DNase I recombinant 10x RNase free (Roche), 5 μL DNase I recombinant 10 U/μL (Roche) and 1 μL Glycogen blue. The samples were then incubated for 2 h at 37ºC and 150 μL of EtOH 100% plus 5 μL of Na^+ Acetate (3 M, pH 5,2) was added in each sample. At this time, the samples were incubated for 30 min at -80ºC, to let the RNA precipitate, and the samples were centrifuged at the maximum rotation at 4ºC for 1 h. The supernatant was discarded and the pellet was one last time washed with 1 mL of EtOH 75%, centrifuged with 7500 xg for 10 min at 4ºC, followed by resuspending, after drying it, with 13 μL of DNase/RNase free water.

The cDNA synthesis was made with the usage of NYZ First-Strand cDNA Synthesis Kit (NZTech). For each condition, the following mix was prepared in sterile, nuclease-free microcentrifuge tubes: 10 μL of NZYRT 2× Master Mix, 200 μg of RNA, and 2 μL of NZYRT Enzyme Mix, making up to 20 μL with DEPC-treated H_2O. As a negative control, one of the samples was not incubated with the Enzyme Mix. The RNA then is incubated at 25°C for 10 min; 50°C for 30 min and 85°C for 5 min and while chilling on ice, 1 μL of NZY RNase H was added and the mix was incubated at 37°C for 20 min. The cDNA product is diluted 1:4 in DNase/RNase-free water.

For the qPCR reaction, is made a technical replicate of n=3 for each condition. In each well, we added 0.7 μL of each primer (used primers in Supplementary Table I.5), 3.6 μL of SybrGreen (Thermo Fisher Scientific), and 5 μL of diluted cDNA product. To confirm that there was not any reaction byproduct, we used a sample with no enzyme mix. *GAPH* was also used as the housekeeping gene to normalize the expression values. The reaction was performed in the ViiA 7 Real-Time PCR System (Thermo Fisher Scientific) in which the settings are referenced in the Supplementary Table I.4. The values were normalized using the $2^{-\Delta Ct}$ method.

2.6 Immunofluorescence Staining

Immunofluorescence (IF) technique is used to assess the expression as well as localization of proteins in the cell through microscopy techniques, resulting in a high-sensitive and high-resolution method of studying cellular components. The experimental setting consists of incubating the sample with a primary antibody and a secondary antibody, that possesses a fluorophore (a molecule that can absorb and emit light with a longer wavelength). This chemical compound is activated using a laser and the signal can be captured and visualized under a fluorescence microscope.

For the analysis of biomarkers of MyoB differentiating to MyoT through the days, the cells were plated in 8 wells plates (μ-Slide 8 Well high Grid-500 (Ibidi) and 4 proteins were detected (the same as the ones used in Section 2.4)). For the analysis of MyoB treated with CM, only the dysferlin was evaluated, so the cells were plated in gridded glass bottom dishes (81166 - iBidi - µ-Dish 35 mm, high Grid-500 ibiTreat). In all cases, the protocol was performed as described below.

The cells were firstly washed twice with 1 mL of PBS-Tween (for the 35 mm dishes it is used a volume of 100 μL). Then they were permeabilized with 1% Triton X-100/PBS for 10 min at RT and washed again twice with PBS-Tween. The cells were blocked by being incubated with PBS-BSA 2% for 30 min at RT and once again washed twice with PBS-Tween. Subsequently, the cells were incubated for 1 h at 37ºC with 100 μL of primary antibodies (for the 8-well plates it is used a volume of 50 μL) with a 1:200 dilution in antibody buffer solution (0.05% TritonX 100, 0.1% sodium azide, 0.2% Fish skin gelatin in PBS 1x) using a humid light-tight box. The incubation with the secondary antibodies (Goat anti-Mouse DyLight™ 488 and Goat anti-rabbit Alexa Fluor™ 488, Thermo Fisher Scientific) was performed with the same dilution and conditions. The samples were further incubated with 4,6-diamidino-2-phenylindole (DAPI) (09542; Sigma Aldrich), a fluorophore that binds to DNA which allows the localization of the nuclei, with a dilution of 1:1000 in PBS 1×, for 10 min at RT. After each incubation, the plates are washed 3 times with 1 mL of PBS-Tween. Finally, the samples were mounted with Fluoromount G (Lab Clinics 00-4958-02).

2.7 Optical and Live-cell microscopy imaging

The brightfield images for comparing physiological differences between conditions were taken in the Primovert optical microscope (Carl Zeiss) with a 4x objective, using a cellphone.

The samples used for IF and FI measurement were visualized by using the Zeiss LSM 880 confocal point-scanning microscope (Carl Zeiss) and using the ZEN Microscopy Software (Carl Zeiss). Image acquisition was performed using a 63x/1.4 oil immersion objective and the ibidi Immersion Oil (Ibidi), compatible with the 8 well plates as well as the gridded glass bottom dishes. The images were taken with a 0.6x zoom with a size of

1024x1024 pixels and a z step of 6,813 μm. The analysis of the images was made using the ImageJ software (version 1.54f).

2.8 Electron Microscopy

The Electron Microscopy (EM) technique uses electrons as a way of obtaining detailed images of cellular components. This technique is based on the property that electrons apply divergence forces to each other. When electrons are emitted to the sample electron-rich components will have an effect on those electrons, scattering them, and so there will be a contrast between the cellular components and the background. Furthermore, variables like thickness and electron composition will affect the signal, allowing the distinction between components. In a simple way, the technique can be divided into 4 different steps: fixation, dehydration, sectioning, and sample imaging.

For these experiments, the MyoT (WT and induced with DNA damage) were washed twice with PBS 1x and fixated using a solution composed of Paraformaldehyde (PFA) 2% and glutaraldehyde 2.5% in 0.1 M phosphate buffer at a temperature of 4ºC. The processing was carried out by the electron microscopy service of the Gulbenkian Institute of Science: The samples were washed twice with 0.1 M phosphate buffer and were centrifuged at 400 xg for 5 min. The cells were washed and centrifuged once more and after that, they were incubated with 1% Osmium tetroxide (OsO_4) in 0.1 M phosphate buffer, on ice for 1 h, in a light-deprived ambiance. The cells were then washed with 0.1 M phosphate buffer for 10 min and washed twice with distilled water for 5 min, each wash. They were incubated one more time with the same conditions as before but this time with 0.5% uranyl acetate at RT, following being washed 3 times with distilled water. The dehydration step was carried out using progressively higher concentrations of ethanol. The infiltration was performed by first applying a 4:1 ethanol/resin mixture for 1 h, at RT, then a 1:4 ethanol/resin mixture at the same conditions with agitation, and lastly a 100% resin incubation, o/n at RT with agitation. The image acquisition was performed using a TEM-FEI G2 Spirit microscope.

2.9 Ultra Performance Liquid Chromatography - Mass Spectrometry

Mass Spectrometry (MS) is a technique that allows the precise identification and quantification of the molecule/protein composition in a sample. This technique ionizes the molecules in the sample so that they can be separated based on the mass-to-charge ratio. This technique can be further paired with others to promote even more precise results. One example is the Liquid Chromatography (LC), which is a separation technique that can be used before doing MS. This technique allows the separation of complex mixtures in a liquid sample. Depending on the technology used (e.g. smaller particle size and higher

pressure) this technique can even further get better performance results, being considered instead Ultra Performance Liquid Chromatography (UPLC).

In order to perform UPLC-MS, the MyoT were induced with DNA damage. The CM of these cells were then collected after waiting 6, 12, and 24 h. For each condition, CM of WT MyoT was also collected.

The samples were sent (in liquid nitrogen), processed, and analyzed by Creative Proteomics. The samples were prepared firstly by being thawed and 1 mL of each was transferred to a new tube. They were lyophilized and it was added 500 μL of 80% methanol, followed by 30 s of vortex and sonication at 4ºC for 30 min. The samples were then incubated at -20ºC for 1 h, being vortexed once more 30 s and incubated at 4ºC for 15 min. They were then centrifuged at 1200 xg at 4ºC for 10 min. It was pipetted 200 μL of the sample together with 5 μL of 0.14 mg/mL DL-o-Chlorophenylalanine to a new vial.

The LC was performed by using Vanquish Flex UPLC with Q Exactive plus MS (Thermo). The ionization was made by Electrospray Ionization (ESI)-MS. The mobile phase is composed of solvent A (0.05% formic acid water) and solvent B (acetonitrile). The gradient elution was 0-1 min, 5% B; 1-12 min, 5%-95% B; 12-13.5 min, 95% B; 13.5-13.6 min, 95%-5% B; 13.6-16 min, 5% B, with a 0.3 mL/min flow rate. The column temperature was 40ºC and the sample manager temperature was 4ºC. The settings for the analysis as well as the parameters for the ESI+ and ESI- mode are listed in the Supplementary table I.1.

2.10 Statistical analysis

For the UPLC-MS samples, the statistical analysis was also performed by Creative Proteomics. The raw data was acquired and aligned using the Compound Discoverer (3.0, Thermo) based on the m/z value and the retention time of the ion signals. Ions from both ESI- and ESI+ are merged and imported into the SIMCA-P program (version 14.1) for multivariate analysis. A Principal Components Analysis (PCA) is first used as an unsupervised method for data visualization and outlier identification. Supervised regression modeling is then performed on the data set by use of Partial Least Squares Discriminant Analysis (PLS-DA) or Orthogonal Partial Least Squares Discriminant Analysis (OPLS-DA) to identify the potential biomarkers. The biomarkers are filtered and confirmed by combining the results of the Variable Importance in Projection (VIP) values (VIP > 1.0) and t-test ($p < 0.05$). The quality of the fitting model can be explained by R2 and Q2 values. A hierarchical cluster analysis was performed of metabolome data from significant metabolites as well as a dot plot of network analysis of the top 25 enriched perturbed metabolites.

3

Results

3.1 Analysis of MyoT nuclei deformation following DNA damage

Unpublished results from the host lab provided some evidence that the MyoT use nuclear autophagy as part of the DDR pathway. To further confirm this evidence, we performed EM to directly observe the damaged muscle cells and assess the formation of nuclear membrane protrusions and vesicle formation inside these cells.

We compared WT MyoT ("Control") with DNA-damaged MyoT ("Treated"). We observe that the majority of control MyoT presented an intact nuclear membrane (Figure 3.1**A**). However, some degree of protrusions could also be observed in some of them (Supplementary Figure II.1**B**). On the other hand, treated MyoT showed a higher number and more severe nuclear membrane deformations. Another characteristic that was observed in treated MyoT was an increased amount of vesicles in the cytoplasm when compared to the control cells (Figure 3.1**B**). Some of the vesicles also seem to possess content inside of them in both conditions, however, they cannot be identified.

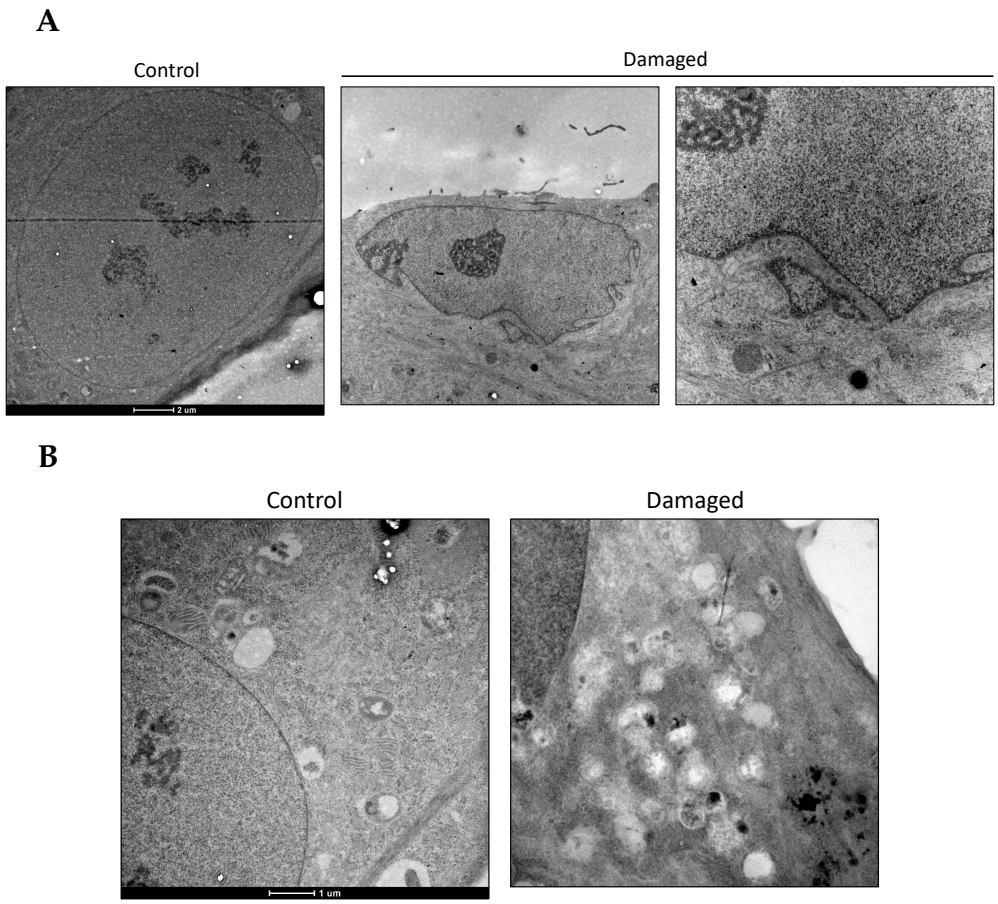

Figure 3.1: MyoT induced with DNA damage shows nuclear membrane protrusions and more vesicles in the cytoplasm. Images obtained by electronic microscopy show MyoT induced with DNA damage ("Damaged") or not ("Control"). In the images, we can observe **(A)** the nuclear membrane and respective protrusions identified by structures with darker outlines and **(B)** the vesicles in the cytoplasm near the nuclear membrane, visualized by white spots in the cell.

3.2 Conditioned medium composition analysis

We wanted to know if, upon DNA damage, the muscle fibers were capable of secreting factors that would activate satellite cells. Therefore, we used UPLC-MS to analyze the composition of the secretome of damaged MyoT. This was made so that we could identify potential factors related to MyoB activation as differentiation, thus further confirming the presence of DASP and better understanding the mechanism behind it.

The respective results were obtained after selecting the compounds that had a VIP > 1 and p-value < 0.05, to filter the ones that were significant. A hierarchical cluster analysis was performed at time points tested (Figure 3.2). The top 25 enriched metabolite sets in the CM of MyoT were used to see which pathways were being perturbed in damaged MyoT. The results are represented as a dot-blot in Figure 3.2. Focusing first on the hierarchical cluster of the 6 h time-point (Figure 3.2**A**), both the ESO+ and ESO- analysis (left and right cluster respectively), we can observe that there is a high quantity of metabolites being more expressed in damaged cells when compared to the control

CM. Amongst them, we have for example the expression of asymmetric dimethylarginine and dihydroneopterin, or diverse types of acids, such as linoleic acid, citraconic acid, and griseolic acid. The treated CM in this condition showed significant variation in the linoleic acid metabolism, in the pentose phosphate pathway, and in the biosynthesis of unsaturated fatty acids, among others. However, it especially showed differences in the starch and sucrose metabolism. Considering the 12 h time-point (Figure 3.2**B**), fewer metabolites showed to be significantly more expressed in damaged cells, having between them molecules such as indoline, reticuline, and glutamine. In these conditions, pathways like purine and tyrosine metabolism showed a high degree of disturbance. With even more significant changes, we have the sulfur metabolism, and once more the biosynthesis of unsaturated fatty acids. Finally, for the 24 h time-point sample (Figure 3.2**C**) metabolites like thymidine, nebracetam, and arginine showed more expression. However, when compared to the other conditions, this one presented more pathways with a significant enrichment. Between them there are pathways of biosynthesis of aminoacyl-tRNA, or in the metabolism of arachidonic, arginine, pyrimidine, and tryptophan, with a highlight in the propanoate metabolism.

A

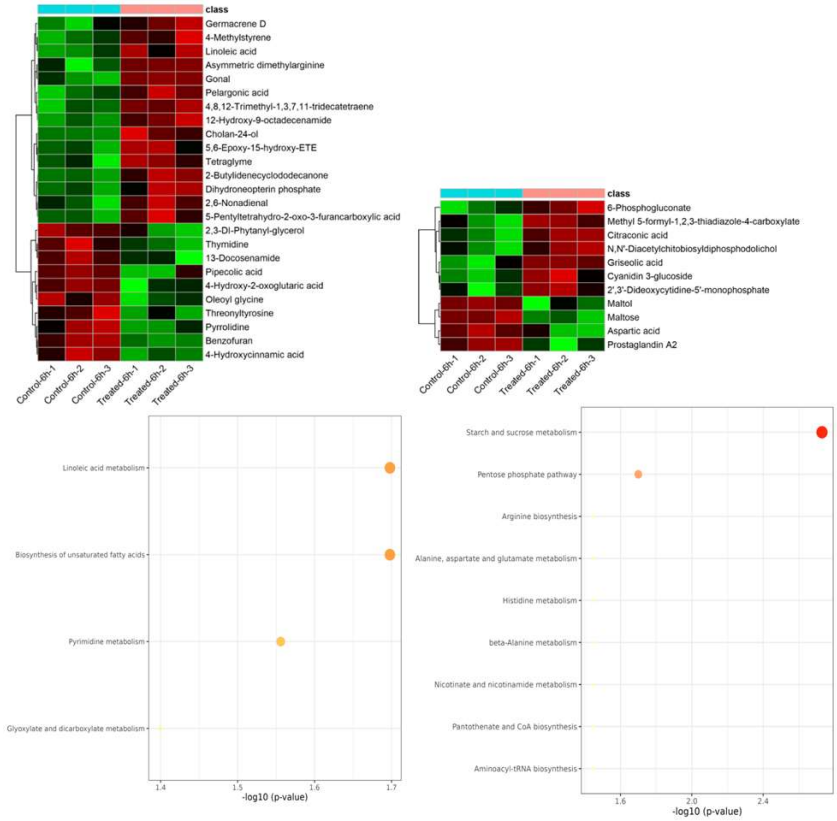
class
Germacrene D
4-Methylstyrene
Linoleic acid
Asymmetric dimethylarginine
Gonal
Pelargonic acid
4,8,12-Trimethyl-1,3,7,11-tridecatetraene
12-Hydroxy-9-octadecenamide
Cholan-24-ol
5,6-Epoxy-15-hydroxy-ETE
Tetraglyme
2-Butylidenecyclododecanone
Dihydroneopterin phosphate
2,6-Nonadienal
5-Pentyltetrahydro-2-oxo-3-furancarboxylic acid
2,3-Di-Phytanyl-glycerol
Thymidine
13-Docosenamide
Pipecolic acid
4-Hydroxy-2-oxoglutaric acid
Oleoyl glycine
Threonyltyrosine
Pyrrolidine
Benzofuran
4-Hydroxycinnamic acid
Control-6h-1
Control-6h-2
Control-6h-3
Treated-6h-1
Treated-6h-2
Treated-6h-3
class
6-Phosphogluconate
Methyl 5-formyl-1,2,3-thiadiazole-4-carboxylate
Citraconic acid
N,N'-Diacetylchitobiosyldiphosphodolichol
Griseolic acid
Cyanidin 3-glucoside
2',3'-Dideoxycytidine-5'-monophosphate
Maltol
Maltose
Aspartic acid
Prostaglandin A2
Linoleic acid metabolism
Biosynthesis of unsaturated fatty acids
Pyrimidine metabolism
Glyoxylate and dicarboxylate metabolism
1.4
1.5
1.6
1.7
-log10 (p-value)
Starch and sucrose metabolism
Pentose phosphate pathway
Arginine biosynthesis
Alanine, aspartate and glutamate metabolism
Histidine metabolism
beta-Alanine metabolism
Nicotinate and nicotinamide metabolism
Pantothenate and CoA biosynthesis
Aminoacyl-tRNA biosynthesis
1.6
2.0
2.4
-log10 (p-value)

B

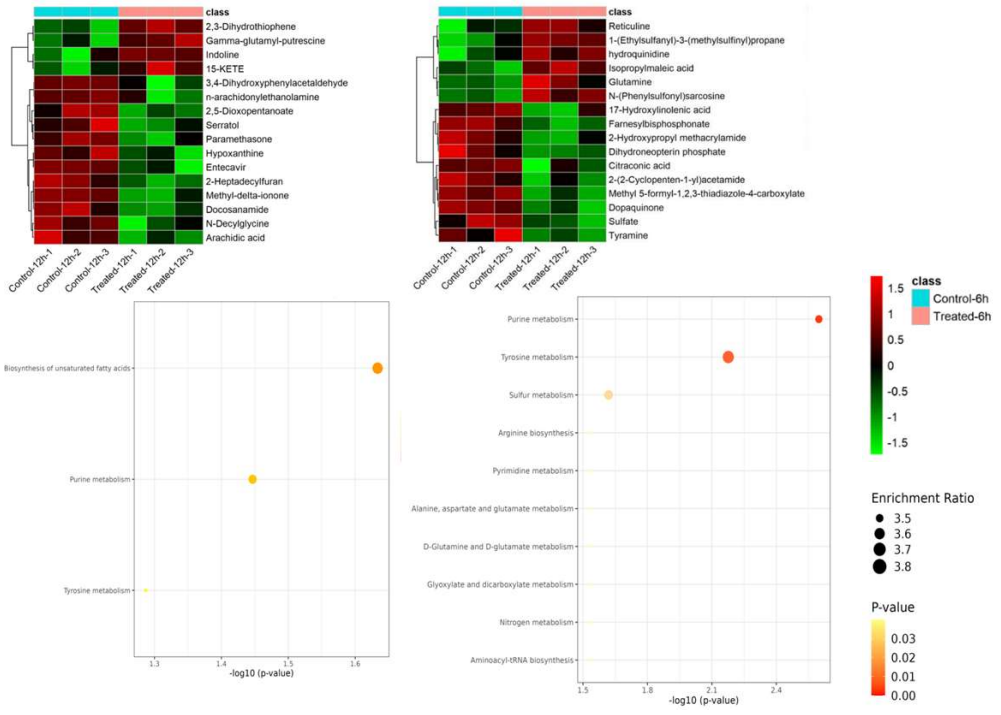
class
2,3-Dihydrothiophene
Gamma-glutamyl-putrescine
Indoline
15-KETE
3,4-Dihydroxyphenylacetaldehyde
n-arachidonylethanolamine
2,5-Dioxopentanoate
Serratol
Paramethasone
Hypoxanthine
Entecavir
2-Heptadecylfuran
Methyl-delta-ionone
Docosanamide
N-Decylglycine
Arachidic acid
Control-12h-1
Control-12h-2
Control-12h-3
Treated-12h-1
Treated-12h-2
Treated-12h-3
class
Reticuline
1-(Ethylsulfanyl)-3-(methylsulfinyl)propane
hydroquinidine
Isopropylmaleic acid
Glutamine
N-(Phenylsulfonyl)sarcosine
17-Hydroxylinolenic acid
Farnesylbisphosphonate
2-Hydroxypropyl methacrylamide
Dihydroneopterin phosphate
Citraconic acid
2-(2-Cyclopenten-1-yl)acetamide
Methyl 5-formyl-1,2,3-thiadiazole-4-carboxylate
Dopaquinone
Sulfate
Tyramine
Biosynthesis of unsaturated fatty acids
Purine metabolism
Tyrosine metabolism
1.3
1.4
1.5
1.6
-log10 (p-value)
Purine metabolism
Tyrosine metabolism
Sulfur metabolism
Arginine biosynthesis
Pyrimidine metabolism
Alanine, aspartate and glutamate metabolism
D-Glutamine and D-glutamate metabolism
Glyoxylate and dicarboxylate metabolism
Nitrogen metabolism
Aminoacyl-tRNA biosynthesis
1.5
1.8
2.1
2.4
-log10 (p-value)
1.5
1
0.5
0
-0.5
-1
-1.5
class
Control-6h
Treated-6h
Enrichment Ratio
3.5
3.6
3.7
3.8
P-value
0.03
0.02
0.01
0.00

C

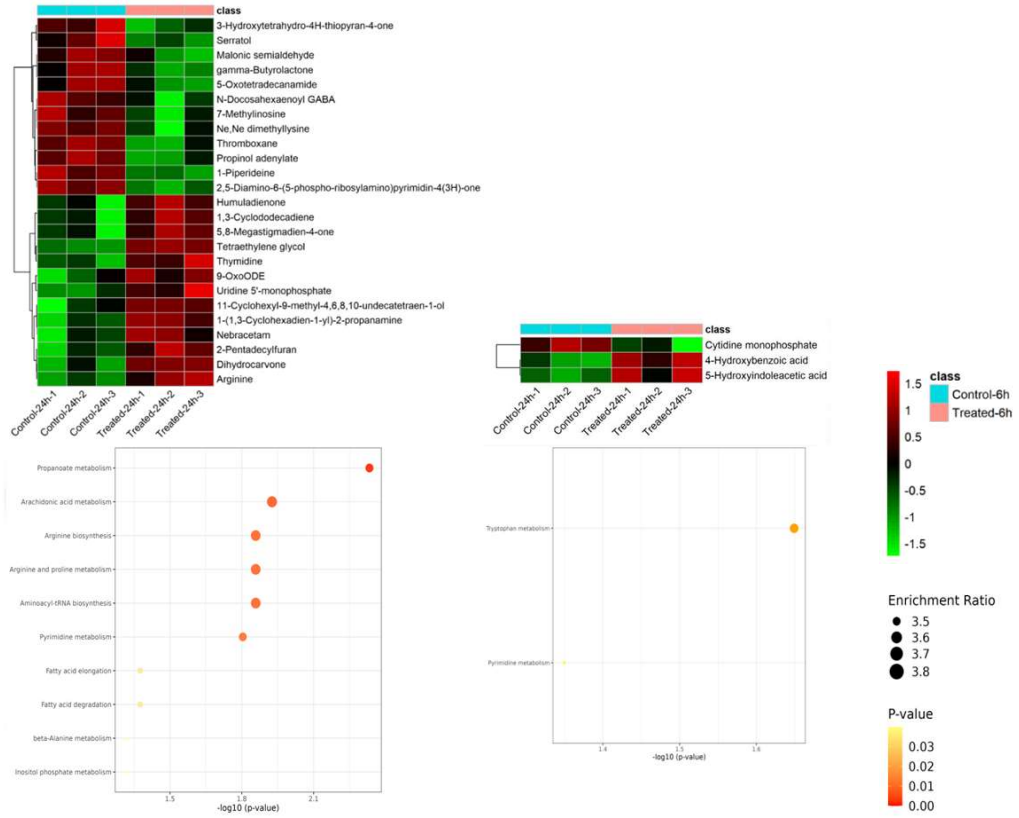

Figure 3.2: The metabolites composition of the secretome of DNA-damaged MyoT are different between time-points. DNA damage was induced to MyoT by treating the cells with NCS. After removing the drug, the CM was collected after **(A)** 6 h, **(B)** 12 h and **(C)** 24 h. The samples were then analyzed by UPLC-MS and the statistical analysis was performed recurring to T-test and PLS-DA analysis. The biomarkers with p-value < 0.05 and VIP > 1 we filtered and considered significant. A hierarchical cluster and a dot plot of network analysis were performed in the filtered metabolites. Results from ESI+ are displayed on the right while the ESI- are displayed on the left.

3.3 Identifying which proteins can be used as biomarkers for MyoB differentiation

In order to see if satellite cells had the capacity to be activated by DNA-damaged myofibers we needed an effective and sensitive way to identify MyoB differentiation. Consequently, we tested several techniques to see which one would better conclude if the MyoB were indeed differentiating. To do that, samples of MyoT were collected at several time points during the differentiation process. All samples were collected every day from day 0 (before starting differentiating) until day 5. Additionally, we also tested different protein markers for cell differentiation, to investigate which one would give the most robust results for us to be able to conclude whether MyoB would fuse or not. For that, we assessed the expression of proteins that have been shown to be involved in muscle cell differentiation (Chapter 1.2.1). Some of these proteins are directly involved in satellite cell activation and differentiation (myogenin and MyHC) while others are biologically part of the muscle cell

structure and are more expressed during differentiation (desmin and dysferlin).

We started by observing the samples under an optical microscope to evaluate any physiological differences between the samples since MyoT have a slightly different physiology when compared to MyoB, which are still not differentiated. MyoT are more elongated and during the process of differentiation, there is an increase in cell death. However, the critical aspect for muscle cells to be considered differentiated is having more cell fusion, thus having more nuclei in each cell. In these images, it is observable that the samples through the days are slightly more elongated (Figure 3.3**A**). Is it not clear when this phenomenon starts to manifest, but there is a difference between days 0 and 5 of differentiation. Moreover, we can observe more cell death (white dots) during the differentiation process. Even though it is uncertain, these changes seem to start to be noticeable on day 2 or 3 of the process. Unfortunately, with these images, it is not possible neither to observe or count the cell nuclei, thus being impossible to directly quantify nuclei fusion between cells.

To better see differences in the expression of the biomarkers through differentiation we performed WB experiments (Figure 3.3**B**). From our results, we can observe an increase in the levels of desmin from day 1 to the following days. For the dysferlin protein marker, it can be observed a small but constant increase of expression through the days. As for the MyHC protein, we observed some small expression starting on day 2 and a strong signal on days 4 and 5, being the last day the one condition with the highest expression. Regarding the myogenin we did not observed a significant signal on any day.

The samples were also analyzed by RT-qPCR since is a more sensitive technique when compared to the WB. We tested the expression of 5 different proteins, four of them being the same as the ones used before, and also MyoD (Figure 3.4). One common characteristic that can be first identified in all samples is that there is always more protein expression on day 5 of differentiation when compared to the samples of initial days (day 0 and day 1). Another common characteristic is that the biggest jump in protein level appears to be between day 1 and day 2. Besides that, the expression levels are different not only during the process but also between the proteins used. The desmin and MyoD proteins showed an increase in expression throughout all differentiation process. On the other hand, dysferlin, MyH3, and myogenin proteins, while their expression increases in the initial days, between day 3 and day 5, the expression decreases.

To analyze the expression by a different method we performed IF experiments. Even though this technique requires more sample preparation, it allows us to directly see the cells and more importantly the cell nuclei, thus allowing us to conclude if the cells are fusing/differentiating by measuring the FI. The images obtained using the dysferlin marker showed us that once more the expression of this protein increased between the days during differentiation (Figure 3.5). Additionally, we can observe a bigger increase in protein expression between day 2 and day 3. Regardless of that, the difference between day 0 and the final day is strikingly clear. More importantly, looking at the DAPI channel, we observe the presence of more multinucleated cells when compared to the initial

days, therefore suggesting MyoT formation. Curiously, the dysferlin signal seems to be increasing not only in the MyoT but also in the MyoB of the same sample (once again, these can be distinguished by clusters of myonuclei that represent MyoT). As for the myogenin marker, a similar result occurs (Figure 3.6): The expression of protein increases through the differentiation days, starting to be more noticeable on day 2. Differently from the dysferlin expression, the signal only appears in the nuclei of the cells. Additionally, the protein expressions appear mostly in the MyoT however, there are some exceptions since there is protein expression in some MyoB (clearly observable on day 0). It can be also seen MyoT formation looking at the DAPI channel.

Using the images of IF, which allows us to identify the myonuclei and therefore distinguish between MyoB and MyoT, we were able to calculate the FI of each sample. This measurement is obtained by calculating the percentage of MyoT nuclei (it is considered a MyoT every cell that has 3 or more nuclei) and dividing by the total nuclei number in the sample (Figure 3.7). By looking at the results, it is obvious that there is an increase in the number of MyoT through the days, agreeing with the previous results. While on day 0 there is a 0% FI, afterward there is a constant increase until reaching values of 75% FI on day 5.

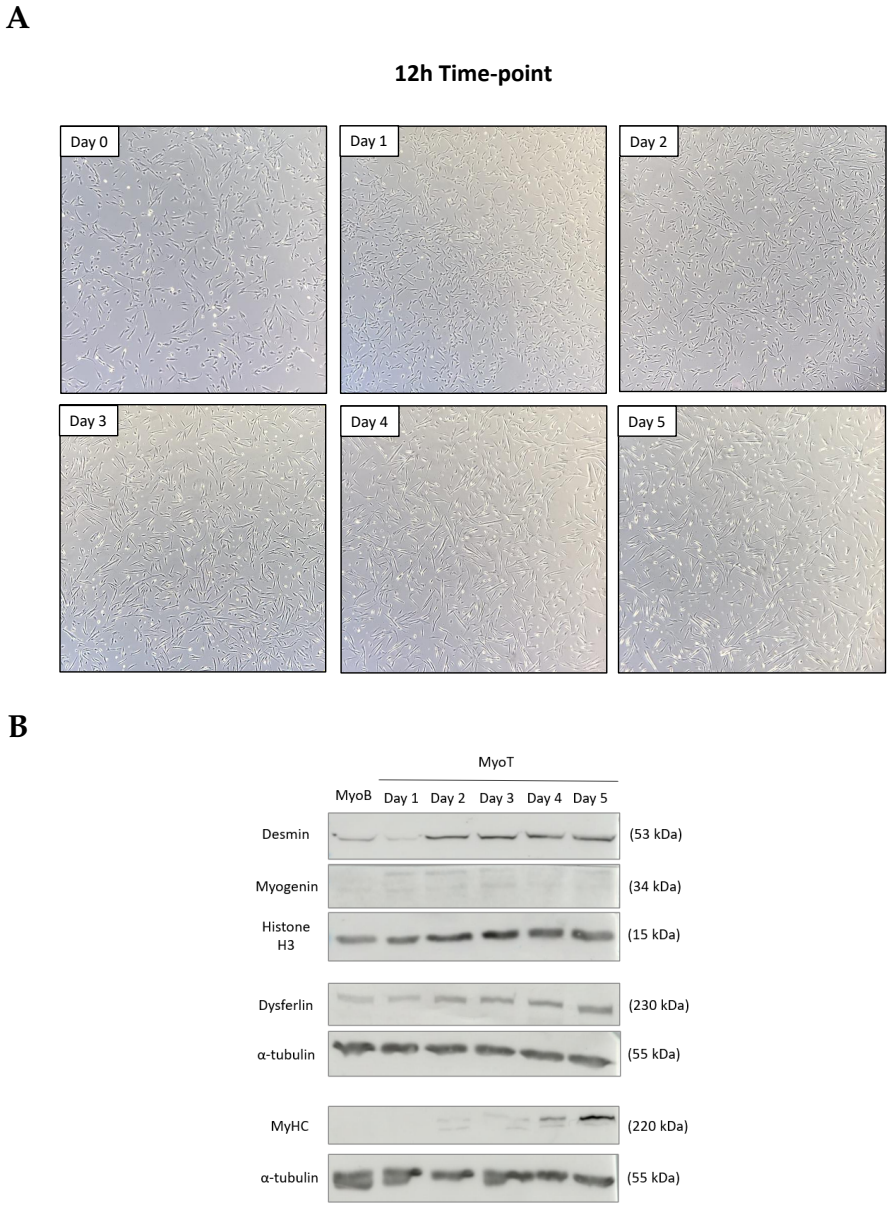

Figure 3.3: During MyoB differentiation to MyoT the cells become more elongated and the expression of the biomarkers increases. Differentiation was induced to KM155 MyoB at a 90% confluency. **A)** Photos taken by optical microscopy with a 4x objective of MyoB with a 50-60% confluency during the process (day 0 to day 5). **B)** WB analysis of differentiation markers. The expression of desmin, dysferlin, and MyHC increases through the differentiation process. The Histone H3 and α-tubulin were used as loading control proteins.

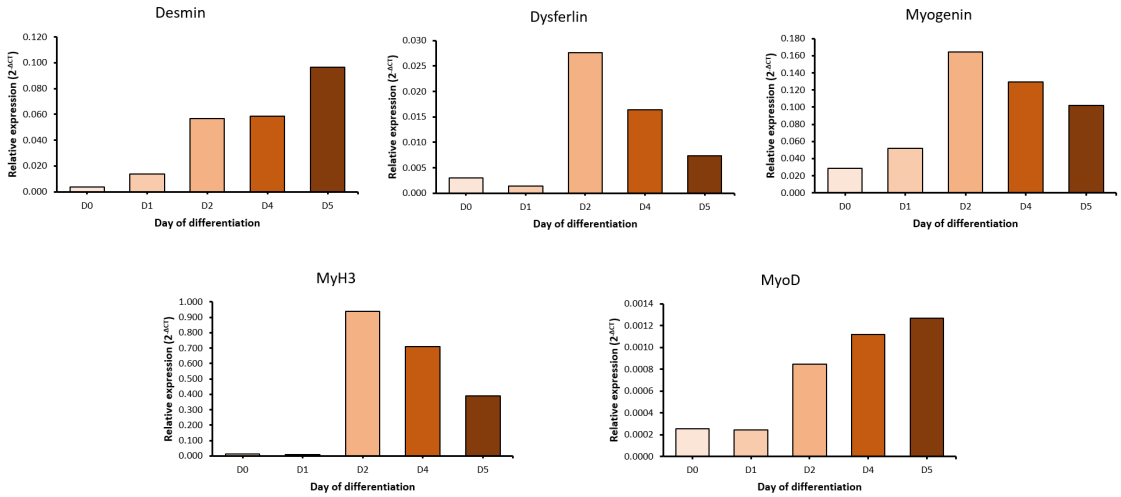

Figure 3.4: Differential expression of skeletal muscle markers during the differentiation process. RT-qPCR analysis of RNA collected from MyoT during the differentiation process (day 0 to 5). The expression of desmin, dysferlin, myogenin (top row), MyH3, and MyoD proteins (bottom row) was evaluated. The x-axis represents each day of differentiation while the y-axis shows the relative expression of each protein, calculated using the $2^{-\Delta Ct}$ method. The samples were normalized using the housekeeping gene *GAPH*.

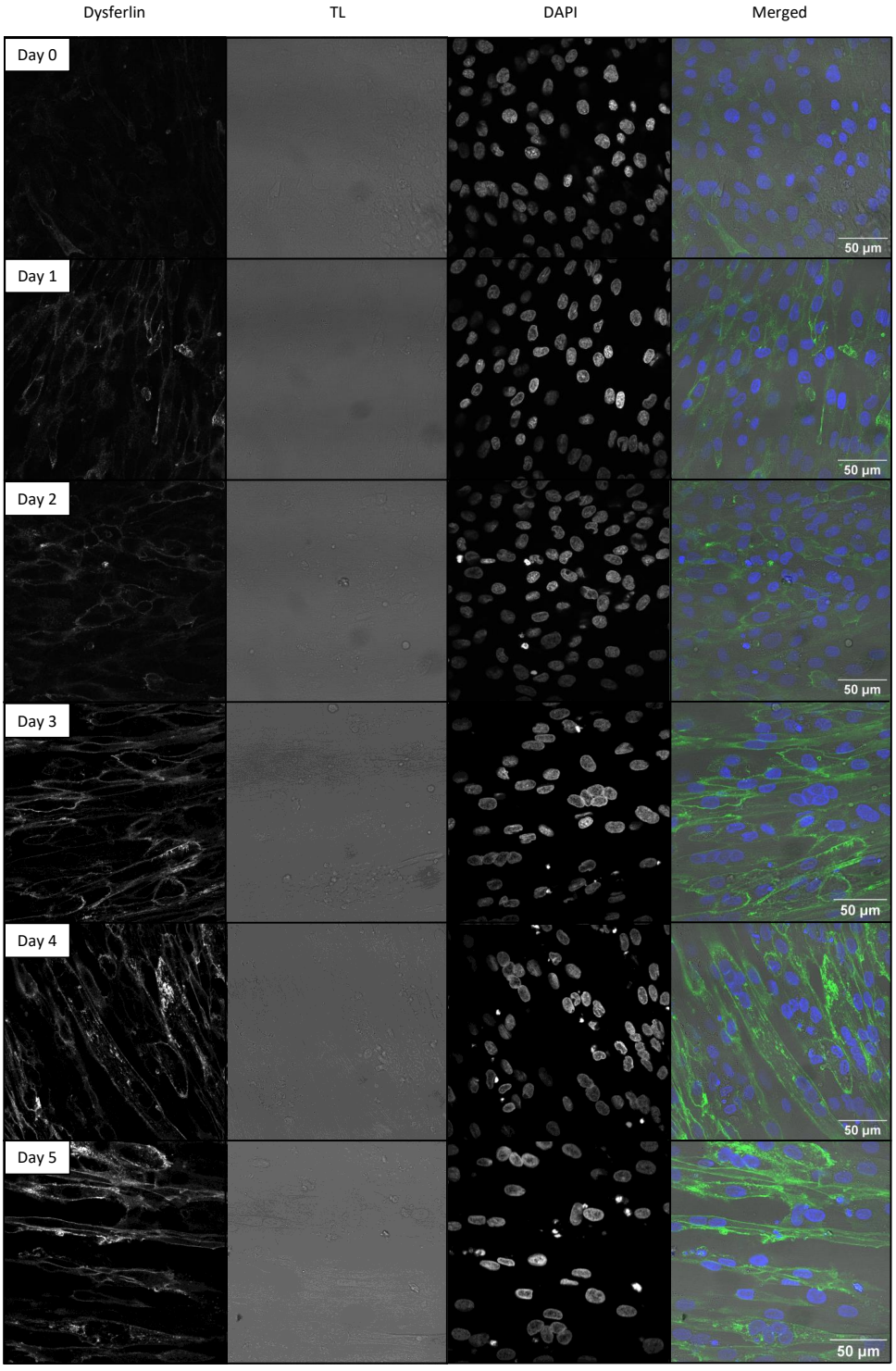

Figure 3.5: The expression of dysferlin increases during differentiation. Representive images from IF assay with an antibody against dysferlin. The MyoB were collected on each day of differentiation, and its analysis is represented in each row (day 0 to day 5). In each column is represented a different channel used for the detection of the same image. From left to right: dysferlin protein expression; Transmitted Light to see the cell outline; DAPI expression to detect the nuclei; final image with the merged channels.

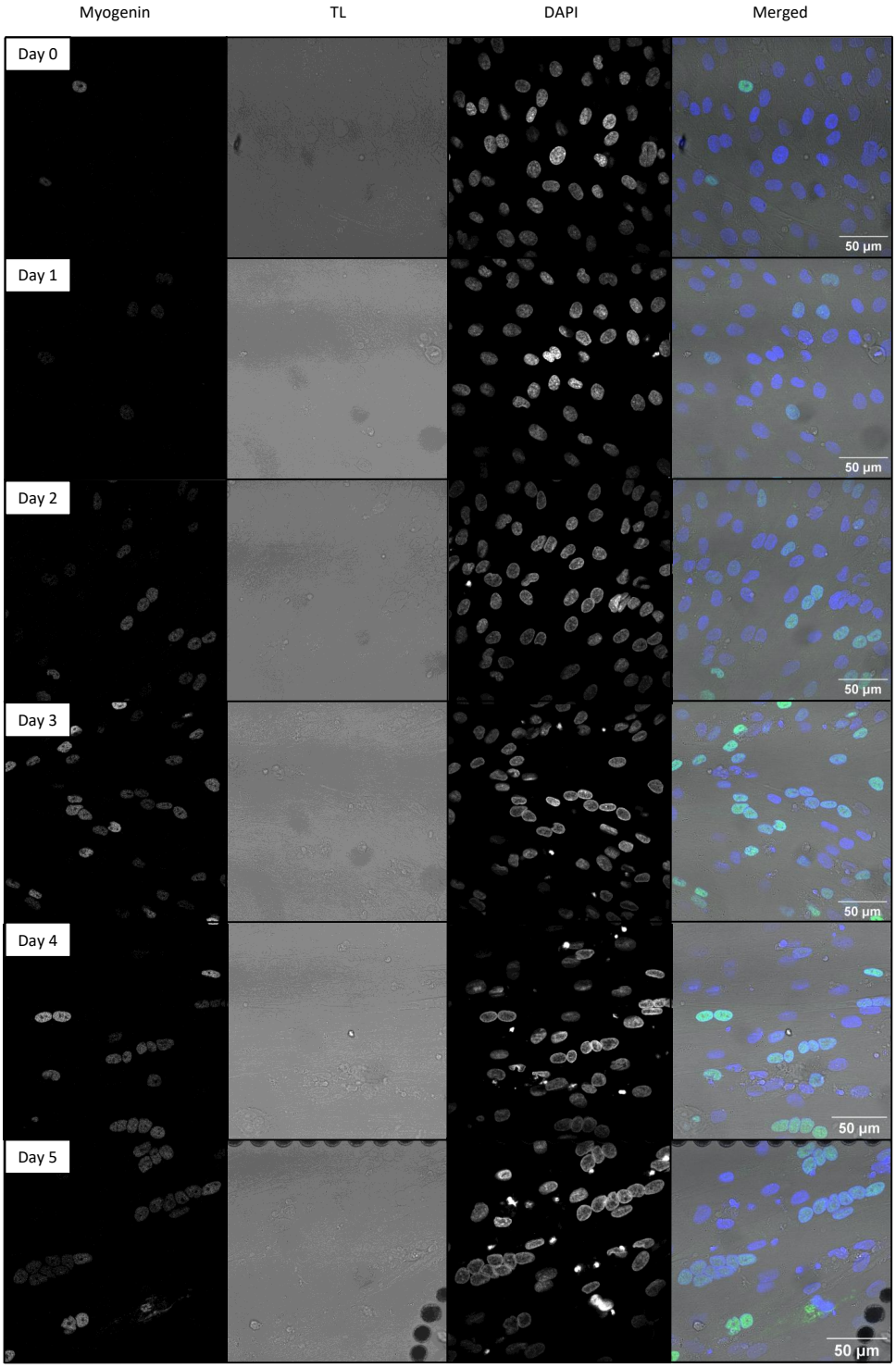

Figure 3.6: The expression of myogenin increases during differentiation. The MyoB were collected on each day of differentiation, and its analysis is represented in each row (day 0 to day 5). Representive images from IF assay with an antibody against myogenin. The MyoB were collected on each day of differentiation, and its analysis is represented in each row (day 0 to day 5). In each column is represented a different channel used for the detection of the same image. From left to right: myogenin protein expression; Transmitted Light to see the cell outline; DAPI expression to detect the nuclei; final image with the merged channels.

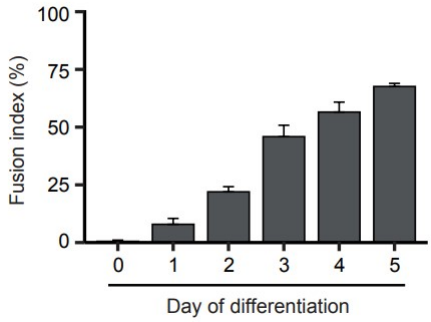

Figure 3.7: The fusion index gradually increases through the differentiation. The BarPlot shows the FI of MyoB, which is calculated by the number of nuclei of MyoT compared to the total number of nuclei in the sample, defined by 3 or more nuclei in the same cell (y-axis). The FI was measured at MyoB at different times of differentiation, between day 0 and day 5 (x-axis). Approximately 500 nuclei were counted.

3.4 Myoblasts response to the conditioned medium of DNA damaged myotubes

After testing which techniques would be suitable for detecting MyoB differentiation, we proceed to evaluate the effects of crosstalk between damaged MyoT and satellite cells. Accordingly, we tested *in vitro* if MyoB would react and differentiate to damaged MyoT by collecting the conditioned medium of damaged MyoT and adding it to the respective MyoB. All the techniques and biomarkers used earlier were also tested in these samples.

Firstly, to confirm if we were indeed inducing DNA damage to MyoT we evaluated the expression of γH2AX, a DNA damage marker in the samples of MyoT treated with NCS, by WB. Both replicates show a higher signal when compared to the control MyoT, confirming DNA damage induction (Supplementary Figure II.2**A**).

Optical microscopy was used to rapidly test many conditions at the same time. The CM was originated from MyoT treated with NCS and collected at different time points after treatment induction (Figure 3.8). Additionally, we decided to test two different approaches. In one group of samples, we added the conditioned medium without medium renewal (NR), while for the other set of samples, we renewed the medium every day throughout the differentiation before collecting the samples (AR). First, we compared phenotypic differences between conditions on day 0 and day 5 of differentiation. Looking at the results for the 6 h time point, we observed that the MyoB NR are more confluent on day 5 without showing signs of differentiation. In the AR condition, the samples on day 5, including the negative control (WT-CM), were really confluent and appeared to have some degree of differentiation, even though it is uncertain. The same happened for the 24 h time point: Even though it looks like the sample on day 5 is more differentiated, when compared with the control, we do not observe a clear difference. This can be due to the fact that the AR conditions are too confluent at all time points tested to understand if they are actually differentiating. Interestingly, the NR samples at the 24 h time points seemed to be more differentiated on day five when compared to day 0. However, between the samples and the control, there were no differences in differentiation level. The MyoB NR treated with dmg-CM showed to be more elongated as well as having more cell death when compared to the negative control (WT-CM) at the 12 h time point. The physiology also seems to be similar to the respective positive control (Figure 3.3**A**), showing a slight increase in elongation and more cell death. Consequently, because the samples seem to be differentiating, the 12 h time point was used for subsequent experiments.

By WB, and using desmin as the marker, it cannot be detected any differences in signal between the MyoB and MyoT (Figure 3.9**A**). The signal of MyoB with CM also seems to be the same as the controls, and the samples in the AR condition are more expressed but are similar to each other. With the dysferlin analysis, we see a small increase in MyoT signal when compared to MyoB, but for the rest of the conditions, either AR or NR, we do not observe much divergence from the controls. The MyoB with a 50-60% confluency which were treated with the CM just for 24 h showed similar results to the results previously

stated (Figure 3.9**B**). We do not observe higher expression of desmin nor dysferlin in the MyoB with dmg-CM when compared with normal MyoB. Considering the MyHC and myogenin, we only observe the expression of these proteins in fully differentiated MyoT. We also wanted to confirm if these results were being caused by DNA damage and not other sources. Therefore, we also induced the damaged MyoT with ATMi to block DNA damage repair. If our hypothesis was correct this would result in a differentiation level increase. However, the sample induced with ATMi also does not show a higher signal than the sample of MyoB with CM or just MyoB. Additionally, MyoT differentiated just for 24 h (positive control) show the same result as the other conditions. However, MyoT fully differentiated presents an increased expression of all differentiation markers. A parallel study was made to detect γH2AX to confirm if the MyoT were getting damaged. Weirdly, damaged MyoT induced with NCS did not show more expression than WT MyoT, used as control (Supplementary Figure II.2**B**).

Interestingly, the results obtained by RT-qPCR were very diverse between biomarkers (Figure 3.9**C**). With the desmin protein, there is more expression in dmg-CM samples, both in NR and AR, when compared to the WT-CM. However, we observe more expression in MyoB rather than in MyoT. In the dysferlin and myogenin, the expression is higher in MyoT than MyoB, being the difference in expression more accentuated in the myogenin samples. While the myogenin shows a small increase in the expression of dmg-CM when compared to WT-CM in both NR and AR samples, the expression with the dysferlin marker shows no differences between WT-CM and dmg-CM. However, there is more expression in the AR samples, when compared to the NR samples. In the MyH3 marker expression, the MyoT also shows way more expression than MyoB as well as more expression in the AR condition when compared to the NR. While WT-CM and dmg-CM do not show differences in the NR condition, there is more expression in the dmg-CM than the other in the AR condition. Finally, even though there is more expression in both dmg-CM than in the WT-CM, the expression in the MyoB is higher than in the MyoT, contrary to what was earlier observed in Figure 3.4.

Once again, the samples were analyzed using IF, since it seems to be the technique that better can identify MyoB differentiation since it directly sees the cell and the respective nuclei while looking at the protein expression (Figure 3.10). In the sample controls, we observe once more a major increase in the dysferlin expression when comparing the MyoB with the MyoT respectively, which goes according to the previous results. When looking into the NR samples' images, it seems that there is little to no protein expression in both samples (dmg-CM and WT-CM). It is also undetectable aggregated nuclei in the same cell when looking into the DAPI expression. The AR dmg-CM and WT-CM samples, on the other hand, both show some degree of expression, which is higher than the NR condition. However, both samples show similar results to one another, having the same dysferlin expression, and this expression does not reach the same level as the positive control (MyoT). Neither the NR nor AR conditions seem to show multinucleated cells.

We then proceed to calculate the FI using the IF images. Our results reveal that the

MyoB samples show no percentage of FI, while the MyoT have an FI of around 50%, confirming that the differentiation was successful (Figure 3.7). Considering both NR and AR conditions, the MyoB treated with dmg-CM showed an FI higher than the WT-CM. However, neither sample has an FI higher than the positive control, not being able to reach an FI higher than 8%. The AR also shows more FI when compared to the samples of NR condition.

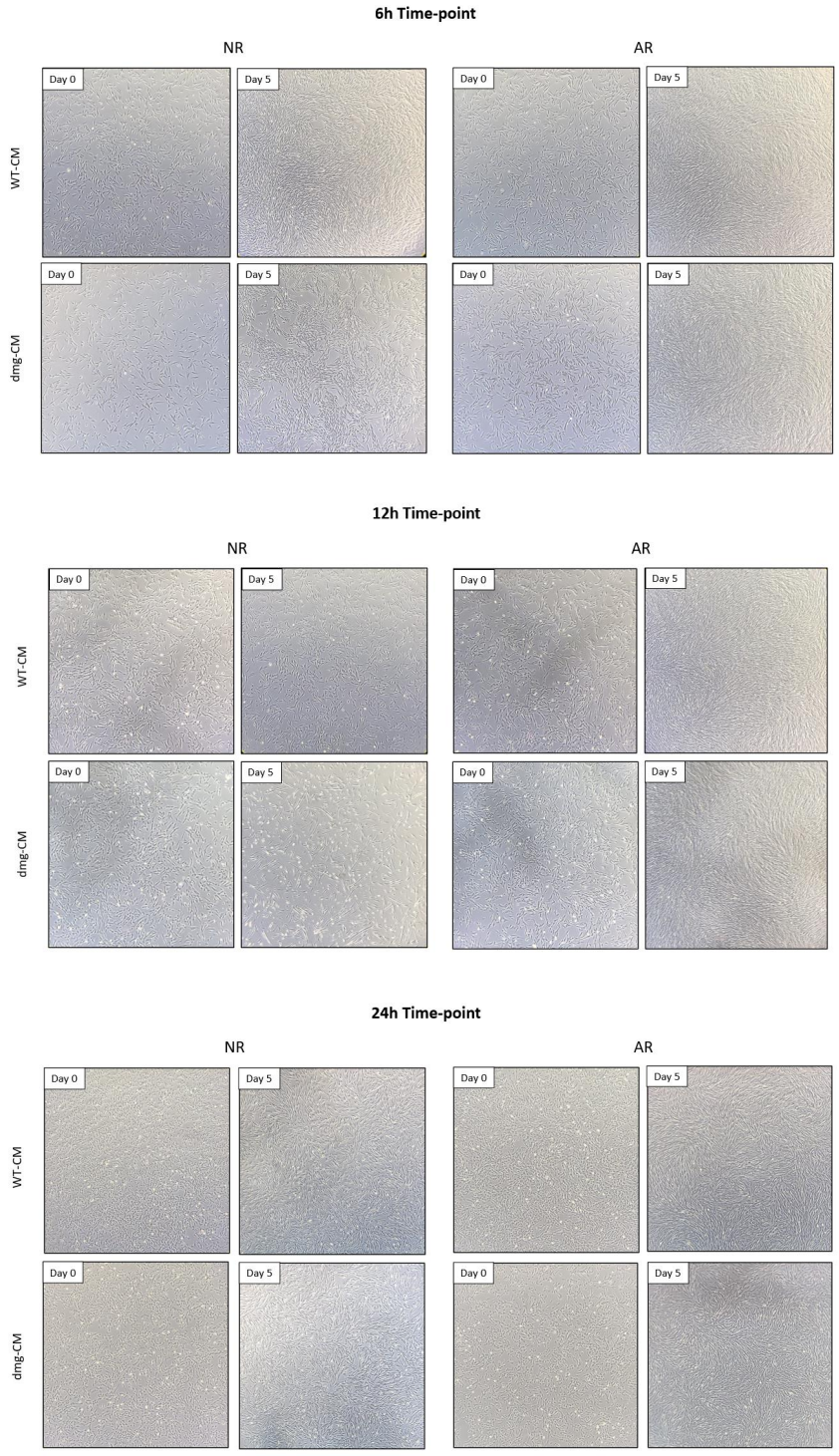

Figure 3.8: MyoB seem to differentiate when in contact with a conditioned medium of DNA damaged MyoT that have been resting for 12 h. Photos taken by an optical microscope with a 4x objective of KM155 cell line with a 50-60% confluency. In each 4-image panel, it can be observed images of MyoB between day 0 (left image) and day 5 (right image) of MyoB treated with a conditioned medium of WT MyoT (top row) and DNA damage Myot (bottom row). The left panel shows MyoB which had the CM just added on the first day and was never renewed (NR), while on the right panel, the MyoB had their CM renewed every day with CM collected from the same MyoT (AR). After being induced with the DNA damage, the MyoT rested for 6 h, 12 h, and 24 h before the CM had been moved to the MyoB.

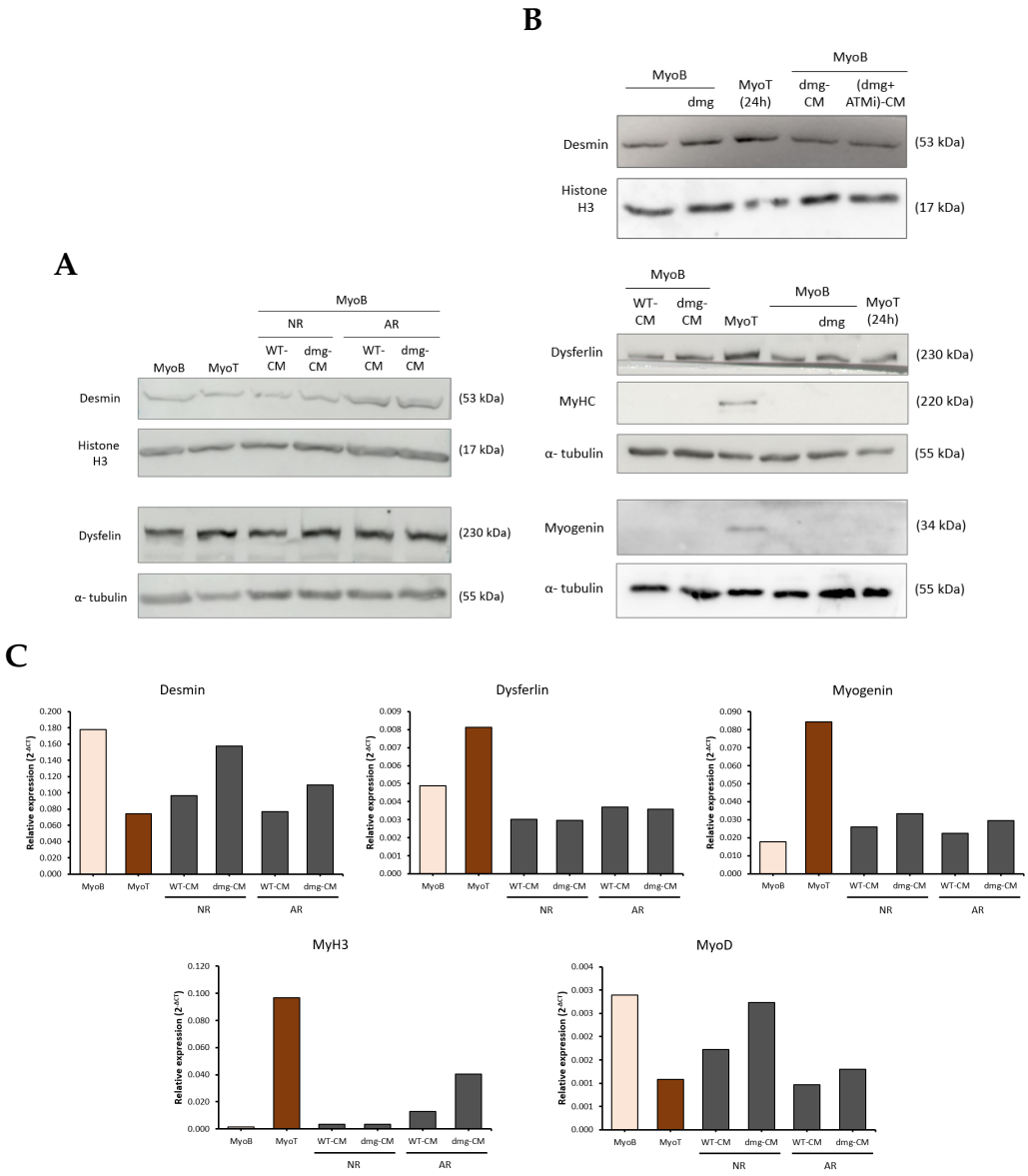

Figure 3.9: Myogenic differentiation markers expression in cells treated with NCS. MyoB were treated with WT-CM and dmg-CM of MyoT. In some samples, the CM was added just on the first day (NR) while in others the CM was renewed every day (AR). MyoB and differentiated MyoT were also analyzed as controls. The cells were analyzed by WB, with the MyoB having **(A)** 50-60% confluency and 5 days with the CM and **(B)** 90% confluency with just 24 h with the CM. In these samples, MyoB were also treated with ATMi. This analysis was made against desmin and myogenin protein expression (12% stacking gel) using Histone H3 as loading control, and dysferlin and MyHC protein expression (6% stacking gel) using α-tubulin as loading control. **(C)** RT-qPCR of RNA collected from the same samples (MyoB at 50-60% confluency and 5 days with the CM). It was used cDNA as template for the PCR, which was made also against desmin, dysferlin, myogenin and MyH3, and also MyoD protein. The expression levels were calculated using the $2^{-\Delta Ct}$ method and they were normalized using the housekeeping gene *DAPH*.

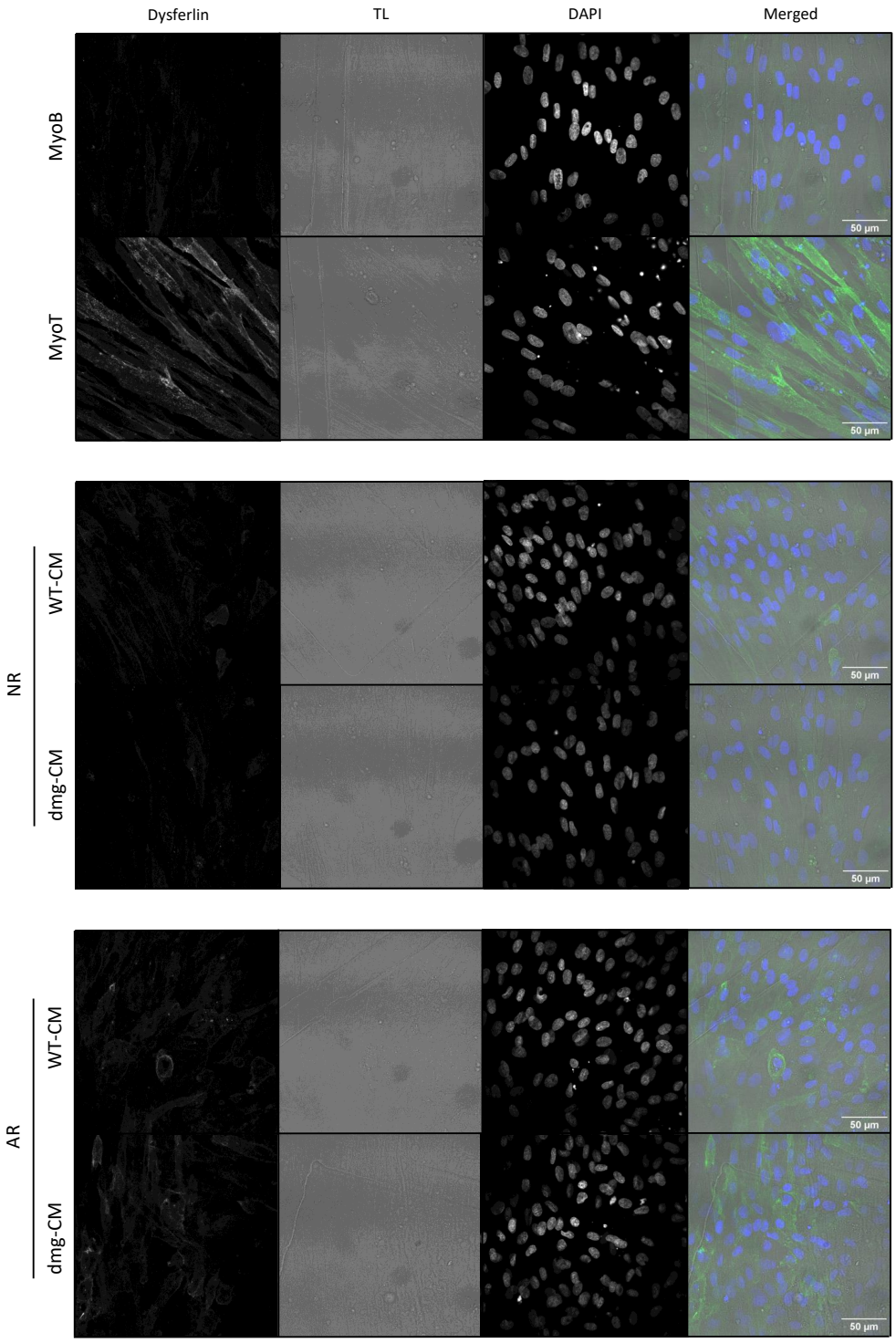

Figure 3.10: Dysferlin expression is higher in AR condition when compared to NR, however, there is no difference between WT-CM and dmg-CM samples. Representative images from IF assay with an antibody against dysferlin. MyoB and differentiated MyoT were used as controls (first set of images). In the other samples, MyoB were treated with WT-CM as well as dmg-CM. In some samples, the CM was added just on the first day (NR; middle set of images) while in others the CM was renewed every day (AR; last set of images). In each column is represented a different channel used for the same image. From left to right: dysferlin protein expression; Transmitted Light to see the cell outline, DAPI expression to detect the nuclei; final image with the merged channels.

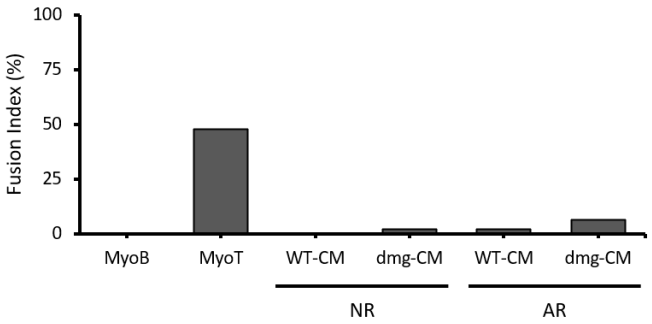

Figure 3.11: There is no relevant increase in FI between WT-CM and dmg-CM MyoB. The BarPlot shows the FI of MyoB, MyoT, and MyoB treated with WT-CM and dmg-CM. In some samples, the CM was added just on the first day (NR) while in others the CM was renewed every day (AR) (x-axis). Approximately 700 nuclei were counted.

4

Discussion

4.1 Effects of DNA damage in MyoT and DDR response by nuclear autophagy

When looking at the EM images of treated MyoT, some of the cells' nuclei show protrusions near the nuclear periphery (Figure 3.1**A**). In some cases, there are even small nuclear envelopes separated from the nuclei themselves. Therefore, these structures could be indicative that there is a compromise of the cells' nuclei due to nuclear autophagy. However, these structures could also just be normal irregularities of the nuclear membrane itself and the ones that are separated from it could be just a consequence of the protocol procedure. Depending on the angle of the sectioning, and because the image was obtained just by using one cut, it is possible that this cut does not capture the rest of the membrane, which might be connected, thus resulting in two distinguished envelopes [102]. Another event that also supports this idea is that, in the control samples, some nuclei showed some grooves near the nuclear membrane that were similar structures to the ones observed in nuclei of the control samples (Supplementary Figure II.1**B**). One possible way of confirming if these structures are being influenced by the sectioning cut is to do a 3D analysis of these cells. With this, we could confirm if indeed it is just a nuclear membrane irregularity or a potential protrusion formation. One way of doing this would be to make a Z-stack analysis of the same samples. This technique analyses multiple section cuts from the same sample area and combines all images to produce a final model.

Regardless of that, it cannot be denied that the damaged MyoT also show an increased number of vesicle formation (Figure 3.1**B**). Even though vesicle formation is essential for the well-functioning of the cell, a higher increase in their number when compared to the control cells, could be indicative that autophagy is indeed happening. However, further experiments need to be made to confirm if these are being induced by autophagy or even nuclear autophagy. One way of supporting this hypothesis would be to analyze vesicles and their content using methods such as heavy metal staining. The presence of genetic material inside the vesicles would be indicative of nuclear autophagy.

4.2 Differences in damaged MyoT medium and secretome composition

By the results obtained by UPLC-MS it was possible to create a hierarchical cluster of the metabolites that were differently expressed when compared between the secretome of normal versus damaged MyoT. By looking at the results, it is clear that the majority of metabolites as well as the pathways of the perturbed metabolites were different between distinct time points (Figure 3.2). This might suggest that the time in which the MyoT are exposed to the NCS influences the type of response that the muscle cells use to repair the DNA damage. This is interesting because the unpublished results from the host lab suggest that muscle cells can repair a certain degree of DNA damage by known methods such as NHEJ, but activate non-canonical pathways when the damage remains unresolved. This can be the moment when nuclear autophagy comes into play and further satellite cells activation occurs. Therefore, we decided to look at the metabolites that appear more in the treated condition and see if there are any reports that correlate these metabolites with muscle cell differentiation. By doing this, we are able to distinguish the different secretome profiles of different time points and clarify which pathway might be involved in the satellite cells activation.

When looking at the time points individually, we see that in the samples of 6 h time point, there is expression of many metabolites, including linoleic acid (Figure 3.2**A**). This compound is an essential saturated fat, meaning that our body cannot synthesize and so it is only intake is by nutrition. However, this fatty acid is provided to the cells in culture by being a component of serum (including Fetal Calf Serum (FCS), which is used for the Skeletal Muscle Cell Media used in this experiment). Additionally, muscle cells are able to store linoleic acid. There have been reports that fatty acids, including linoleic acid, can induce muscle cell proliferation as well as differentiation. Not only that, there are suspicions that Extracellular Signal-regulated Kinase 1/2 (ERK1/2) may contribute to the fatty acid-induced differentiation since cells incubated with them showed higher levels of ERK1/2 [103]. These two proteins are part of the Mitogen-Activated Protein Kinase (MAPK) signaling pathway, which receives extracellular signals and activates a signal cascade that will regulate different cell mechanisms, and between them, cell differentiation [104]. We can also observe in the dot plot that the metabolism of linoleic acid is one of the most enriched sets, further magnifying its importance in the DDR of treated cells. Interestingly, there is also an enrichment of the biosynthesis of unsaturated fatty acids, which are the key component for the formation of cell membranes. This could be an indication that treated cells are forming more vesicles. If the DASP mechanism uses vesicles as a way for secreting satellite cells activation factors, this could suggest that DNA-damaged MyoT are activating satellite cells. Interestingly, even though the starch and sucrose metabolism is one of the most enriched pathways, there are no reports that relate these molecules to muscle differentiation.

Looking now to the 12 h time point condition (Figure 3.2**B**), one metabolite that drew

attention was the upregulation of glutamine. This is because l-glutamine has been shown to increase MyoB differentiation by promoting the expression of differentiation proteins, like myogenin, igf-1, MyHC 2 & 7, etc [105]. This protein changes the MAPK pathway, via p38. The dot plot also shows a higher disturbance in the biosynthesis of unsaturated fatty acids, which goes along with the previous results. However, there is a big enrichment in the tyrosine and purine metabolism. This is interesting since microtubule structures, the ones that are induced by purine, have been shown to perturb muscle cell differentiation when these are inhibited [106]. Moreover, in that context, the cells become unresponsive to cell differentiation queues, thus showing that purine-based microtubules are necessary for this process [107]. Additionally, tyrosine kinases also have been shown to be induced during muscle cell differentiation and tyrosine phosphatase has been shown to inhibit cell growth also during differentiation [108].

Lastly, the 24 h time point condition shows different metabolite profiles than the other two conditions (Figure 3.2**C**). One metabolite that has shown to be predominant in the hierarchy cluster and dot plot was the arginine. Even though there is not much research correlating this molecule with muscle differentiation, there are studies reporting that arginine methyltransferase is necessary for muscle differentiation, by the activation of mef2 [109]. Additionally, its inhibition promotes the decrease of the differentiation protein myogenin, further reinforcing its role in muscle differentiation. Interestingly, there are also reports of arginine methyltransferase promoting MyoB differentiation by regulating the expression of p38, which is involved in the MAPK pathway [110]. At this time point, there are many pathways that seem to be enriched, especially the propanoate metabolism. However, these do not have support material that relates them to muscle differentiation. Indeed, many metabolites that are more expressed in MyoT might not be involved with differentiation, but are just part of the cells regular metabolism. This is due to the fact that the sample is composed of all conditioned medium of MyoT and not only composed of DDR secretome. It is certain that this is a limitation of this experimental setting.

All conditions show us some promising results. Between the many metabolites that are being more expressed in damaged MyoT, some of them seem to directly affect the differentiation of muscle cells. There is also an inclination of these metabolites towards specific pathways, which is the case of the MAPK pathway. This signaling pathway is involved in critical processes for muscle cells, like cell survival, proliferation, and differentiation. However, to further better identify the mechanism behind DASP satellite cell activation it would be optimal to make a proteomic analysis and correlate the respective results with the previous ones. This would be also beneficial to understand the different profiles between time points. Once there is a strong suggestion that a certain pathway is involved in the DASP mechanism, inhibiting that pathway and seeing if MyoB have the same response would be critical to confirm the hypothesis.

4.3 DASP consequences in MyoB

The methods used to identify MyoB differentiation gave us different results altogether. Optical microscopy photos showed us some physiological changes in the cells that were noticeable through the differentiation days (Figure 3.3**A**). These changes were accordingly of what was expected: The cells were more elongated, which is a strong sign that they are being differentiated, and also showed more cell death, which even though is not directly related to the MyoT formation, is known that, during the process of differentiation, there is an increase in cell death [111]. However, these characteristics by themselves are not enough to confirm that the MyoB are indeed differentiating, especially because we are not directly looking at nuclei fusion. This is important because multinucleation is a distinctive feature of mature MyoT. An important factor that might be influencing our results and the respective conclusions is cell confluency, which by itself influences myoblast fusion. In this work, the samples were analyzed with a confluency of around 50-60%. Because of the low cell density, the cells hardly reached one another, making it difficult to form more elongated cells. The difference is more prominent when we compared the control obtained with an example of MyoT cells fully differentiated with a confluency of 90%, which shows longer cells forming fibers-like patterns (Supplementary Figure II.1**A**). Unfortunately, we could not increase the confluency of the samples because MyoB, when they reach a certain cell density level, they start to fuse with each other without the need for an additional stimulus, leading to false positive results. One example of this would be the results obtained of the MyoB AR either treated with WT-CM or dmg-CM, in all time points. When we look into the images (Figure 3.8), we observe that on day 5 the cells indeed seem to be differentiating, since they are more elongated. However, this could be provoked by the proliferation and consequent high confluency of these cells. Thus, it would be crucial to optimize this parameter in the experimental procedure itself. Since we did not know if the agents supposedly secreted would be enough of a trigger cell differentiation, and at the time they would be secreted, we decided to constantly have the agents in contact with the MyoB (AR condition). However, the medium that was being renewed every day consisted of Growth Medium. We theorize that because the MyoB were being treated with the fresh CM containing Growth Medium, the cells were growing at a faster rate, thus becoming confluent in a short period of time. Regardless, it could be that these samples show some differences between the dmg-CM and the WT-CM, however, these cannot be detectable by this approach. On the other hand, the same did not happen in the NR samples. The MyoB with dmg-CM samples at the 6 and 24 h time points show some increase in the confluency, however did not appear to be elongated. While looking into the 12 h time point, the cells appear to be differentiating since, when compared to the WT-CM samples, the cells have more cell death and are slightly more elongated. Because of this, we selected this time point for subsequent analysis.

When looking at the WB results (Figure 3.3**B**), we can conclude that the desmin, dysferlin, and MyHC protein markers originate similar results of what was expected: The

two first proteins work as early differentiation markers and slightly increase through the differentiation days, while MyHC works as a late differentiation marker, not expressing in the first days but showing signal in later stages of differentiation. Dysferlin, however, seems to be the optimal biomarker to identify MyoB differentiation because the desmin signal fluctuates between days while repeating the experiment. Since it only expresses in later days, MyHC might also not be optimal to identify differentiation in earlier days or small fusion between cells. Regardless, desmin and MyHC might help compare big changes in differentiation levels. The MyoB treated with dmg-CM does not seem to show increased expression of dysferlin when compared to the controls (Figure 3.9**A**). Adding to that, the samples of MyoB NR also do not present higher levels of desmin expression but they do show more expression on the AR samples when compared to the controls. However, the MyoT do not show more expression than the MyoB, which should be expected. Still looking at the desmin results, The MyoB AR are more expressed than the rest conditions, which can be explained once more by the samples' confluency that are forcing the MyoB to differentiate. However, it does not justify the MyoT having a small expression. Two factors can be influencing these results: cell confluency and the degree of DNA damage. The low confluency of the cells may impair cell fusion. Another possible explanation is that the MyoT are not being damaged or the damage in the MyoT is not strong enough to induce nuclear autophagy and the secretory phenotype of MyoT. As referenced before, we believe that NHEJ can deal with the majority of damage in the cells and that nuclear autophagy is used only after a certain damage threshold. Indeed, when testing the level of γH2AX of MyoT, while MyoT induced with NCS analyzed in Figure 3.9**A**, had more γH2AX expression, damaged MyoT analyzed in Figure 3.9**B** show even lesser damage than the control MyoT (Supplementary Figure II.2). This suggests that the drug used in that experiment might not been working properly and that this might be the explanation for why the MyoB are not being activated. The other results show the same expression levels of MyoB treated with dmg-CM with the negative control (MyoB) (Figure 3.9**B**). The levels in the positive control however are higher than the other bands probably because in these experiments the confluency of the samples was around 90%. This might be allowing the cells to be proximal to each other or might even be mechanically stressing the MyoB to fuse. Moreover, the addition of ATMi had the purpose of inhibiting ATM and shutting the DDR pathway in the MyoT. If our hypothesis is correct and the DDR is involved in muscle cell regeneration, there would be more activation of satellite cells (more MyoB differentiation). Following the same results as the other samples, the expression level also did not alter in this condition. Altogether these results suggest that MyoB differentiation is not evident in the conditions analyzed. However, we strongly think that WB might not be the most optimal method to identify differentiation since it is not sensitive enough to identify small differentiation levels between samples.

Opposite to WB which is a more qualitative method, RT-qPCR is a quantitative method that is more sensitive. With this method we reached the same conclusion regarding the expression of differentiation markers during MyoT differentiation: There is more

expression on day 5 when compared to day 0 (Figure 3.4). While in the desmin, dysferlin, myogenin, and MyH3 this should be expected, the MyoD protein is a transcription factor that appears only during earlier stages of differentiation, being absent in terminally differentiated muscle cells [112]. Surprisingly, MyoD shows to be steadily increasing through the days, which does not follow what would be expected. Another occurring characteristic is that there is a big increase between day 1 and day 2 of differentiation. This was somewhat expected since all methods (optical microscopy, WB, or IF) show that the MyoB actually start to differentiate/fuse during day 2 and 3. What we were not expecting is that the signal, in the majority of cases (dysferlin, myogenin, and MyH3), starts to decrease. This is especially unexpected in the case of later differentiation markers such as myogenin and MyH3. When we compared these results to the MyoB and MyoT samples used in the MyoB treated with CM, some of the markers showed opposite expressions (Figure 3.9**C**). For example, the desmin and MyoD show more expression in the MyoB when compared to the MyoT. In the case of the expression of MyoD it shows similar results to what is reported in the literature. Surprisingly, when looking at the MyoB treated with CM, we can observe increased expression of desmin, myogenin, and MyoD in the samples treated with dmg-CM than the ones treated with WT-CM, both in NR and AR conditions. In the MyH3 there is also more expression of dmg-CM but only in the AR MyoB. This result is somewhat expected since MyH3 is only expressed in later stages of differentiation, and as observed in the optical microscopy experiments, these conditions are more confluent which can influence the differentiation process. These results concur with our hypothesis, however, to have a definitive conclusion there is the need to perform more replicates. Several factors may be influencing the variability in results observed in control samples, including the limited number of replicates and the cell confluency level. While in MyoT differentiation was induced when the samples had a 90% confluency, the MyoB treated with CM were only at 50-60% confluency at the time that differentiation was induced. Moreover, we observe some variance between samples in the levels of the housekeeping gene *GAPH* which could also affect the results. A future solution to resolve this issue would be to use another housekeeping gene, such as U6.

The results obtained by IF were clearer. It is obvious that the number of positive cells constantly increases through the days of differentiation either in dysferlin or myogenin (Figure 3.5 and 3.6). Since dysferlin is a membrane protein, the signal seems to delimit the cells while in the myogenin, which is a nuclear protein, the signal only appears in the nuclei. Another interesting result is that while in the dysferlin the signal shows to be more intense through the days and affects all cells in general, the myogenin signal only appears in nuclei that are fused. When looking at the MyoB that were treated with CM (Figure 3.10), is it obvious that there is no difference between the samples treated with dmg-CM and WT-CM, either in NR or AR samples. Here, we also observe that the signal seems to be higher in the AR condition when compared to the MyoB, which is in agreement with the results that were obtained before. Once more, we reason that this is probably caused by the cells' growth. Differently from the results obtained in the WB, the positive control

sample (MyoT with 50-60% confluency) was able to differentiate. So, these results suggest that confluency might not be the problem in this case, but rather the MyoB do not actually differentiate. The signal might not be strong enough to induce differentiation, or there is no damage in the MyoT responsible for the CM (as explained previously). Regardless, this technique shows to be one of the most optimal, since we can directly look at the signal at the cells. However, the most useful characteristic of the method is being able to directly see the cells' nuclei (like it can be observed in the DAPI channel). Since the nuclei of MyoT usually appear next to each other and we are also able to see the cells' delimitation, it is relatively easy to see directly which cells are actually differentiating. This also allows us to measure the FI, which shows a steady increase through differentiation.

When looking at the FI of our conditions, it seems that there is more differentiation in the MyoB treated with dmg-CM than with WT-CM (Figure 3.11). However, neither condition seems to have an FI nearly close to the MyoT, which has a FI of around 50% (lower than the sample in Figure 3.7, which is expected due to the lower confluency), while the rest of the samples do not surpass an 8% confluency. Therefore, it is not possible to draw a conclusion and more replicates need to be made to confirm these results. However, even though the MyoB have a low confluency, the dmg-CM samples still show some degree of differentiation when compared to WT-CM. The analysis by IF and the measure of FI using these images seems to be the most optimal method to investigate MyoB differentiation. However, the protocol can still be optimized. One of the problems we encountered was the bias when obtaining the photos. The cells do not grow evenly in the plate and the distinct confluency of the cells in different places of the plate might influence differentiation. While some areas might have not enough cells to be able to fuse to one another, others might be more confluent and the cells can fuse because they are stressed. In the areas with higher confluency, it was also difficult to assess if two nuclei close together belonged to the same cell or not.

In general, it is difficult to have a definite conclusion if MyoB indeed differentiate upon being treated with dmg-CM. Photos taken by optical microscopy were really helpful in testing different conditions in a short period of time and it was a good first indicator if the MyoB were reacting to the CM as it happened in the 12 h time point. However, other methods like WB were not good at identifying any differences, maybe due to the trigger not being strong enough. The RT-qPCR showed indeed MyoB differentiation but more replicates need to be done to be fully sure. Other housekeeping genes would also be advised. Besides having some setbacks, by far the most reliable techniques were indeed the IF and the consequent FI calculation, since both can directly identify nuclei fusion. Corroborating with our hypothesis, these techniques seem to indicate that there might be MyoB differentiation due to DNA damage. However, a lot of optimizations need to be done to the experimental protocol in order to reach a definite conclusion. One of the optimizations required is related to cell confluence as cells that have low confluency may not be close enough to start to fuse. On the other hand, having too much confluency can by itself promote MyoB differentiation. Moreover, we might not be seeing an effect because

the trigger might not also be strong enough to induce MyoB activation and differentiation. We reason that MyoT only resort to DASP if the lesion cannot be repaired by the canonical DNA repair mechanisms, and the concentration of NCS used in this study might not be enough to cause such deleterious lesions. To test this hypothesis, it would be interesting to induce DSB by increasing the level of NCS used. Another thing that could be made is to test other drugs to see if they induce different effects on the MyoT and MyoB response. It would be also interesting to inhibit the NHEJ pathway in muscle cells to make them resort only to nuclear autophagy to repair their DNA. Regardless of all that, dysferlin was shown to be the most reliable protein to show persistent results across all techniques used, being a good candidate to be used as an early differentiation biomarker.

4.4 Future perspectives

As for future experiments, it would be optimal to further study the MyoT CM. In addition to analyzing the enriched metabolism, it would also be advantageous to study the proteomic of the same conditions, in order to better understand the mechanism behind DASP. Once we had a general idea of which pathway or group of pathways the DASP uses, targeting those specific pathways would also be a good next step to better understand the mechanism.

We started testing the experiments in simple models like the MyoB, to avoid as many variables as possible. However, satellite cells activation might only work on more complex models. Therefore, future experiments using *in vivo* models would also be advised. This is due to the fact that the DASP mechanism might only work in more complex structures, such as the satellite cells niche and myofibers.

Another interesting experiment would be to see if the DASP mechanism preceded changes during aging. As discussed in the introduction, aging has an evident impact on DNA stability and it is correlated with muscle-deficient regeneration. One of the consequences or causes could be the ineffective mechanism of DASP in older people. This could be studied by looking at the DASP mechanism and satellite cells activation in age-related conditions such as Hutchinson–Gilford progeria syndrome-induced mice.

5

Conclusions

Corroborating with previous data, this work strongly indicates that MyoT, which are DNA damage induced, might use nuclear autophagy as a way to repair DNA damage. This is mainly supported by the increased number of vesicles in these cells. This work also shows some metabolites that are strongly related to muscle cell differentiation pathways. Therefore, we suggest that the damaged MyoT secrete agents that will activate satellite cells, a mechanism which we denominated DASP. However, it is still difficult to determine whether the MyoB treated with these agents can be activated, thus differentiating. Besides the protocol optimizations made, a few counter-steps still need to be resolved. Between them we have the cells' confluency, which can lead to false positive results; dosage and drug type; trigger for inducing damage; and simplicity of the model used. Overtaking these issues and understanding better the mechanism behind DASP would increase our knowledge about cell DDR complexity in skeletal muscle fibers.

Bibliography

[1] J. M. Lourenço. *The NOVAthesis LaTeX Template User's Manual*. NOVA University Lisbon. 2021. URL: https://github.com/joaomlourenco/novathesis/raw/main/template.pdf (cit. on p. i).

[2] I. Faleiro et al. "Adaptive Changes in the DNA Damage Response During Skeletal Muscle Cell Differentiation". In: *Cell and Developmental Biology* (2023). DOI: 10.3389/fcell.2023.1239138 (cit. on p. iii).

[3] B. Rydberg. *Clusters of DNA Damage Induced by Ionizing Radiation: Formation of Short DNA Fragments. II. Experimental Detection*. 1996, pp. 200–209 (cit. on p. 1).

[4] K. Machida et al. "Hepatitis C Virus Triggers Mitochondrial Permeability Transition with Production of Reactive Oxygen Species, Leading to DNA Damage and STAT3 Activation". In: *Journal of Virology* 80.14 (2006), pp. 7199–7207. DOI: 10.1128/jvi.00321-06 (cit. on p. 1).

[5] R. T. Pomerantz and M. O'Donnell. *What happens when replication and transcription complexes collide?* 2010-07. DOI: 10.4161/cc.9.13.12122 (cit. on p. 1).

[6] F. Prado and A. Aguilera. "Impairment of replication fork progression mediates RNA polII transcription-associated recombination". In: *EMBO Journal* 24 (6 2005-03), pp. 1267–1276. ISSN: 02614189. DOI: 10.1038/sj.emboj.7600602 (cit. on p. 1).

[7] N. Chatterjee and G. C. Walker. "Mechanisms of DNA damage, repair, and mutagenesis". In: *Environ Mol Mutagen* 58.5 (2017-05), pp. 235–263. DOI: 10.1002/em.22087 (cit. on p. 2).

[8] W. P. Roos and B. Kaina. "DNA damage-induced cell death: From specific DNA lesions to the DNA damage response and apoptosis". In: *Cancer Letters* 332.2 (2013). Apoptosis Targeting Drugs in Cancer, pp. 237–248. ISSN: 0304-3835. DOI: https://doi.org/10.1016/j.canlet.2012.01.007 (cit. on p. 2).

[9] A. P. Del Vesco et al. "Age-related oxidative stress and antioxidant capacity in heat-stressed broilers". In: *animal* 11.10 (2017), pp. 1783–1790. DOI: 10.1017/S1751731117000386 (cit. on p. 2).

[10] R. Agrelo et al. *Epigenetic inactivation of the premature aging Werner syndrome gene in human cancer*. 2006 (cit. on p. 2).

[11] A. Vítor et al. "Studying DNA Double-Strand Break Repair: An Ever-Growing Toolbox". In: *Frontiers in Molecular Biosciences* 7 (2020-02). DOI: 10.3389/fmolb.2020.00024 (cit. on p. 2).

[12] K. Edo et al. "The structure of neocarzinostatin chromophore possessing a novel bicyclo-[7,3,0]dodecadiyne system". In: *Tetrahedron Letters* 26.3 (1985), pp. 331–334. ISSN: 0040-4039. DOI: https://doi.org/10.1016/S0040-4039(01)80810-8 (cit. on p. 2).

[13] I. H. Goldberg. "Mechanism of neocarzinostatin action: role of DNA microstructure in determination of chemistry of bistranded oxidative damage". In: *Accounts of Chemical Research* 24.7 (1991), pp. 191–198. DOI: 10.1021/ar00007a001 (cit. on p. 3).

[14] C. T. Carson et al. "The Mre11 complex is required for ATM activation and the G2/M checkpoint". In: *The EMBO Journal* 22.24 (2003), pp. 6610–6620. DOI: https://doi.org/10.1093/emboj/cdg630 (cit. on p. 3).

[15] J. Falck, J. Coates, and S. P. Jackson. "Conserved modes of recruitment of ATM, ATR and DNA-PKcs to sites of DNA damage". In: *Nature* 434.7033 (2005-03), pp. 605–611. ISSN: 0028-0836. DOI: 10.1038/nature03442 (cit. on p. 3).

[16] A. Kinner et al. "γ-H2AX in recognition and signaling of DNA double-strand breaks in the context of chromatin". In: *Nucleic Acids Research* 36 (2008), pp. 5678–5694 (cit. on p. 3).

[17] J. Tang et al. "Acetylation Limits 53BP1 Association with Damaged Chromatin to Promote Homologous Recombination". In: *Nature structural molecular biology* 20 (2013-02). DOI: 10.1038/nsmb.2499 (cit. on p. 3).

[18] P.-O. Mari et al. "Dynamic assembly of end-joining complexes requires interaction between Ku70/80 and XRCC4". In: *Proceedings of the National Academy of Sciences* 103.49 (2006), pp. 18597–18602. DOI: 10.1073/pnas.0609061103 (cit. on p. 3).

[19] J. Walker, R. Corpina, and J. Goldberg. "Structure of the Ku heterodimer bound to DNA and its implications for double-strand break repair". In: *Nature* 412.6847 (2001-08), pp. 607–614. ISSN: 0028-0836. DOI: 10.1038/35088000 (cit. on p. 3).

[20] N. Uematsu et al. "Autophosphorylation of DNA-PKCS regulates its dynamics at DNA double-strand breaks ". In: *Journal of Cell Biology* 177.2 (2007-04), pp. 219–229. ISSN: 0021-9525. DOI: 10.1083/jcb.200608077 (cit. on p. 3).

[21] Y. Ma et al. "Hairpin Opening and Overhang Processing by an Artemis/DNA-Dependent Protein Kinase Complex in Nonhomologous End Joining and V(D)J Recombination". In: *Cell* 108.6 (2002), pp. 781–794. ISSN: 0092-8674. DOI: https://doi.org/10.1016/S0092-8674(02)00671-2 (cit. on p. 3).

[22] J. Perry et al. "WRN exonuclease structure and molecular mechanism imply an editing role in DNA end processing". In: *Nature structural molecular biology* 13 (2006-06), pp. 414–22. DOI: 10.1038/nsmb1088 (cit. on p. 3).

[23] S. Li et al. "Polynucleotide Kinase and Aprataxin-like Forkhead-associated Protein (PALF) Acts as Both a Single-stranded DNA Endonuclease and a Single-Stranded DNA 3 Exonuclease and Can Participate in DNA End Joining in a Biochemical System*". In: *The Journal of Biological Chemistry* 286 (2011), pp. 36368–36377 (cit. on p. 3).

[24] U. Grawunder et al. *Activity of DNA ligase IV stimulated by complex formation with XRCC4 protein in mammalian cells*. 1997 (cit. on p. 3).

[25] P. Fiorentini et al. "Exonuclease I of Saccharomyces cerevisiae Functions in Mitotic Recombination In Vivo and In Vitro". In: *Molecular and cellular biology* 17 (1997-06), pp. 2764–73. DOI: 10.1128/MCB.17.5.2764 (cit. on p. 3).

[26] M. Clerici et al. "The Saccharomyces cerevisiae Sae2 Protein Promotes Resection and Bridging of Double Strand Break Ends*". In: *Journal of Biological Chemistry* 280.46 (2005), pp. 38631–38638. ISSN: 0021-9258. DOI: https://doi.org/10.1074/jbc.M508339200 (cit. on p. 3).

[27] A. L. Eggler, R. B. Inman, and M. M. Cox. "The Rad51-dependent Pairing of Long DNA Substrates Is Stabilized by Replication Protein A*". In: *Journal of Biological Chemistry* 277.42 (2002), pp. 39280–39288. ISSN: 0021-9258. DOI: https://doi.org/10.1074/jbc.M204328200 (cit. on p. 3).

[28] "BRCA1–BARD1 Activates RAD51 for DNA Repair by Homologous Recombination". In: *Cancer Discovery* 7.12 (2017-12), OF6–OF6. ISSN: 2159-8274. DOI: 10.1158/2159-8290.CD-RW2017-195 (cit. on p. 3).

[29] M. Tarsounas, D. Davies, and S. West. "BRCA2-dependent and independent formation of RAD51 nuclear foci". In: *Oncogene* 22 (2003-03), pp. 1115–23. DOI: 10.1038/sj.onc.1206263 (cit. on p. 3).

[30] J. Neal et al. "Inhibition of Homologous Recombination by DNA-Dependent Protein Kinase Requires Kinase Activity, Is Titratable, and Is Modulated by Autophosphorylation". In: *Molecular and cellular biology* 31 (2011-02), pp. 1719–33. DOI: 10.1128/MCB.01298-10 (cit. on p. 4).

[31] Z. Mao et al. "Comparison of nonhomologous end joining and homologous recombination in human cells". In: *DNA repair* 7 (2008-09), pp. 1765–71. DOI: 10.1016/j.dnarep.2008.06.018 (cit. on p. 4).

[32] A. S. Zhiyong Mao Michael Bozzella and V. Gorbunova. "DNA repair by nonhomologous end joining and homologous recombination during cell cycle in human cells". In: *Cell Cycle* 7.18 (2008), pp. 2902–2906. DOI: 10.4161/cc.7.18.6679 (cit. on p. 4).

[33] H. H. Chang et al. *Non-homologous DNA end joining and alternative pathways to double-strand break repair*. 2017-08. DOI: 10.1038/nrm.2017.48 (cit. on p. 5).

[34] R. D. Johnson and M. Jasin. "Sister chromatid gene conversion is a prominent double-strand break repair pathway in mammalian cells". In: *The EMBO Journal* 19 (2000) (cit. on p. 5).

[35] O. Limbo et al. "Ctp1 Is a Cell-Cycle-Regulated Protein that Functions with Mre11 Complex to Control Double-Strand Break Repair by Homologous Recombination". In: *Molecular Cell* 28.1 (2007), pp. 134–146. ISSN: 1097-2765. DOI: https://doi.org/10.1016/j.molcel.2007.09.009 (cit. on p. 5).

[36] D. Yilmaz et al. "Activation of homologous recombination in G1 preserves centromeric integrity". In: *Nature* 600 (2021-12). DOI: 10.1038/s41586-021-04200-z (cit. on p. 5).

[37] M. Van Sluis and B. Mcstay. "A localized nucleolar DNA damage response facilitates recruitment of the homology-directed repair machinery independent of cell cycle stage". In: *Genes Development* 29 (2015-06). DOI: 10.1101/gad.260703.115 (cit. on p. 5).

[38] A. Sallmyr and A. E. Tomkinson. "Repair of DNA double-strand breaks by mammalian alternative end-joining pathways". In: *J Biol Chem* 293.27 (2018-03), pp. 10536–10546. DOI: 10.1074/jbc.TM117.000375 (cit. on p. 5).

[39] W. R. Frontera and J. Ochala. "Skeletal muscle: a brief review of structure and function". In: *Calcified tissue international* 96.3 (2015-03), pp. 183–195. ISSN: 0171-967X. DOI: 10.1007/s00223-014-9915-y (cit. on p. 5).

[40] E. Reichl et al. "Interactions between Myosin and Actin Crosslinkers Control Cytokinesis Contractility Dynamics and Mechanics". In: *Current biology : CB* 18 (2008-05), pp. 471–80. DOI: 10.1016/j.cub.2008.02.056 (cit. on p. 5).

[41] J. M. Squire. "Architecture and function in the muscle sarcomere". In: *Current Opinion in Structural Biology* 7.2 (1997), pp. 247–257. ISSN: 0959-440X. DOI: https://doi.org/10.1016/S0959-440X(97)80033-4 (cit. on p. 5).

[42] S. Tajbakhsh et al. "Redefining the Genetic Hierarchies Controlling Skeletal Myogenesis: Pax-3 and Myf-5 Act Upstream of MyoD". In: *Cell* 89 (1997), pp. 127–138. URL: https://api.semanticscholar.org/CorpusID:18747744 (cit. on p. 6).

[43] M. Rudnicki et al. "MyoD or Myf-5 is required for the formation of skeletal muscle". In: *Cell* 75 (1994-01), pp. 1351–9. DOI: 10.1016/0092-8674(93)90621-V (cit. on p. 6).

[44] R. N. Cooper et al. "In vivo satellite cell activation via Myf5 and MyoD in regenerating mouse skeletal muscle". In: *Journal of Cell Science* 112.17 (1999-09), pp. 2895–2901. ISSN: 0021-9533. DOI: 10.1242/jcs.112.17.2895 (cit. on p. 6).

[45] B. Friday et al. "Calcineurin initiates skeletal muscle differentiation by activating MEF2 and MyoD". In: *Differentiation* 71.3 (2003), pp. 217–227. ISSN: 0301-4681. DOI: https://doi.org/10.1046/j.1432-0436.2003.710303.x (cit. on p. 6).

[46] B. Nadal-Ginard. "Commitment, fusion and biochemical differentiation of a myogenic cell line in the absence of DNA synthesis". In: *Cell* 15.3 (1978), pp. 855–864. ISSN: 0092-8674. DOI: https://doi.org/10.1016/0092-8674(78)90270-2 (cit. on p. 6).

[47] Z. L. Li and D. Paulin. "High level desmin expression depends on a muscle-specific enhancer." In: *Journal of Biological Chemistry* 266.10 (1991), pp. 6562–6570. ISSN: 0021-9258. DOI: https://doi.org/10.1016/S0021-9258(18)38154-7 (cit. on p. 7).

[48] N. de Luna, E. Gallardo, and I. Illa. "In Vivo and In Vitro Dysferlin Expression in Human Muscle Satellite Cells". In: *Journal of Neuropathology Experimental Neurology* 63.10 (2004-10), pp. 1104–1113. ISSN: 0022-3069. DOI: 10.1093/jnen/63.10.1104 (cit. on p. 7).

[49] J. Matheny Ronald W. and B. C. Nindl. "Loss of IGF-IEa or IGF-IEb Impairs Myogenic Differentiation". In: *Endocrinology* 152.5 (2011-05), pp. 1923–1934. ISSN: 0013-7227. DOI: 10.1210/en.2010-1279 (cit. on p. 7).

[50] C. F. Bentzinger et al. "Cellular dynamics in the muscle satellite cell niche". In: *EMBO reports* 14.12 (2013), pp. 1062–1072. DOI: https://doi.org/10.1038/embor.2013.182 (cit. on p. 7).

[51] J. Gros et al. "A common somitic origin for embryonic muscle progenitors and satellite cells". In: *Nature* 435 (7044 2005-06), pp. 954–958. ISSN: 00280836. DOI: 10.1038/nature03572 (cit. on p. 7).

[52] T. Hurme and H. O. Kalimo. "Activation of myogenic precursor cells after muscle injury." In: *Medicine and science in sports and exercise* 24 2 (1992), pp. 197–205. URL: https://api.semanticscholar.org/CorpusID:10076595 (cit. on p. 8).

[53] "Stem cell function, self-renewal, and behavioral heterogeneity of cells from the adult muscle satellite cell niche". In: *Cell* 122 (2 2005-07), pp. 289–301. ISSN: 00928674. DOI: 10.1016/j.cell.2005.05.010 (cit. on p. 8).

[54] P. Rocheteau, M. Vinet, and F. Chretien. "Dormancy and Quiescence of Skeletal Muscle Stem Cells". In: *Vertebrate Myogenesis: Stem Cells and Precursors*. Ed. by B. Brand-Saberi. Berlin, Heidelberg: Springer Berlin Heidelberg, 2015, pp. 215–235. ISBN: 978-3-662-44608-9. DOI: 10.1007/978-3-662-44608-9_10 (cit. on p. 8).

[55] J. Sanes. "The Basement Membrane/Basal Lamina of Skeletal Muscle". In: *The Journal of biological chemistry* 278 (2003-05), pp. 12601–4. DOI: 10.1074/jbc.R200027200 (cit. on p. 8).

[56] A. A. Cutler et al. "The regenerating skeletal muscle niche drives satellite cell return to quiescence". In: *iScience* 25.6 (2022), p. 104444. ISSN: 2589-0042. DOI: https://doi.org/10.1016/j.isci.2022.104444 (cit. on p. 8).

[57] F. Lazure et al. "Transcriptional Reprogramming of Skeletal Muscle Stem Cells by the Niche Environment". In: *bioRxiv* (2021). DOI: 10.1101/2021.05.25.445621 (cit. on p. 8).

[58] R. Bischoff. "Interaction between satellite cells and skeletal muscle fibers". In: *Development* 109.4 (1990-08), pp. 943–952. ISSN: 0950-1991. DOI: 10.1242/dev.109.4.943 (cit. on p. 8).

[59] R. Tatsumi et al. "HGF/SF Is Present in Normal Adult Skeletal Muscle and Is Capable of Activating Satellite Cells". In: *Developmental Biology* 194.1 (1998), pp. 114–128. ISSN: 0012-1606. DOI: https://doi.org/10.1006/dbio.1997.8803 (cit. on p. 8).

[60] W. Roman and P. Muñoz-Cánoves. "Muscle is a stage, and cells and factors are merely players". In: *Trends in Cell Biology* 32.10 (2022), pp. 835–840. ISSN: 0962-8924. DOI: https://doi.org/10.1016/j.tcb.2022.03.001 (cit. on p. 8).

[61] Y. Kharraz et al. "Macrophage Plasticity and the Role of Inflammation in Skeletal Muscle Repair". In: *Mediators of inflammation* 2013 (2013-01), p. 491497. DOI: 10.1155/2013/491497 (cit. on p. 8).

[62] J. Tidball and A. Villalta. "Regulatory interactions between muscle and the immune system during muscle regeneration". In: *American journal of physiology. Regulatory, integrative and comparative physiology* 298 (2010-03), R1173–87. DOI: 10.1152/ajpregu.00735.2009 (cit. on p. 8).

[63] "DNA repair byproduct 8-oxoguanine base promotes myoblast differentiation". In: *Redox Biology* 61 (2023), p. 102634. ISSN: 2213-2317. DOI: https://doi.org/10.1016/j.redox.2023.102634 (cit. on p. 8).

[64] "PDGF-B secreted from skeletal muscle enhances myoblast proliferation and myotube maturation via activation of the PDGFR signaling cascade". In: *Biochemical and Biophysical Research Communications* 639 (2023), pp. 169–175. ISSN: 0006-291X. DOI: https://doi.org/10.1016/j.bbrc.2022.11.085 (cit. on p. 8).

[65] J. E. Anderson. "A Role for Nitric Oxide in Muscle Repair: Nitric Oxide–mediated Activation of Muscle Satellite Cells". In: *Molecular Biology of the Cell* 11.5 (2000). PMID: 10793157, pp. 1859–1874. DOI: 10.1091/mbc.11.5.1859 (cit. on p. 8).

[66] R. Tatsumi et al. "Satellite cell activation in stretched skeletal muscle and the role of nitric oxide and hepatocyte growth factor". In: *American Journal of Physiology-Cell Physiology* 290.6 (2006). PMID: 16684931, pp. C1487–C1494. DOI: 10.1152/ajpcell.00513.2005 (cit. on p. 8).

[67] M. Hill, A. Wernig, and G. Goldspink. "Muscle satellite (stem) cell activation during local tissue injury and repair". In: *Journal of Anatomy* 203.1 (2003), pp. 89–99. DOI: https://doi.org/10.1046/j.1469-7580.2003.00195.x (cit. on p. 8).

[68] T. Floss, H. H. Arnold, and T. Braun. "A role for FGF-6 in skeletal muscle regeneration". In: *Genes and Development* 11 (16 1997-08), pp. 2040–2051. ISSN: 08909369. DOI: 10.1101/gad.11.16.2040 (cit. on p. 8).

[69] J. Jeong, M. Conboy, and I. Conboy. "Pharmacological inhibition of myostatin/TGF-β receptor/pSmad3 signaling rescues muscle regenerative responses in mouse model of type 1 diabetes". In: *Acta pharmacologica Sinica* 34 (2013-06). DOI: 10.1038/aps.2013.67 (cit. on p. 8).

[70] S. Watanabe et al. "Skeletal muscle releases extracellular vesicles with distinct protein and microRNA signatures that function in the muscle microenvironment". In: *PNAS Nexus* 1.4 (2022-08), pgac173. ISSN: 2752-6542. DOI: 10.1093/pnasnexus/pgac173 (cit. on p. 9).

[71] A. Forterre et al. "Myotube-derived exosomal miRNAs downregulate Sirtuin1 in myoblasts during muscle cell differentiation". In: *Cell cycle (Georgetown, Tex.)* 13 (2013-10). DOI: 10.4161/cc.26808 (cit. on p. 9).

[72] S. Ji et al. "Myoblast-derived exosomes promote the repair and regeneration of injured skeletal muscle in mice". In: *FEBS Open Bio* 12.12 (2022), pp. 2213–2226. DOI: https://doi.org/10.1002/2211-5463.13504 (cit. on p. 9).

[73] M.-C. Le Bihan et al. "In-depth analysis of the secretome identifies three major independent secretory pathways in differentiating human myoblasts". In: *Journal of Proteomics* 21 (2011-12), pp. 344–56. DOI: 10.1016/j.jprot.2012.09.008 (cit. on p. 9).

[74] M. Raab et al. "ESCRT III repairs nuclear envelope ruptures during cell migration to limit DNA damage and cell death". In: *Science* 352.6283 (2016), pp. 359–362. DOI: 10.1126/science.aad7611 (cit. on p. 9).

[75] E. Barbieri and P. Sestili. "Reactive oxygen species in skeletal muscle signaling". In: *Journal of Signal Transduction* 2012 (2012), pp. 1–17. DOI: 10.1155/2012/982794 (cit. on p. 9).

[76] T. Nouspikel and P. C. Hanawalt. "DNA repair in terminally differentiated cells". In: *DNA Repair* 1.1 (2002), pp. 59–75. ISSN: 1568-7864. DOI: https://doi.org/10.1016/S1568-7864(01)00005-2 (cit. on pp. 9, 10).

[77] L. Narciso et al. "Terminally differentiated muscle cells are defective in base excision DNA repair and hypersensitive to oxygen injury". In: *Proceedings of the National Academy of Sciences* 104 (2007), pp. 17010–17015. URL: https://api.semanticscholar.org/CorpusID:19468284 (cit. on p. 10).

[78] C. van der Wees et al. "Nucleotide excision repair in differentiated cells". In: *Mutation Research/Fundamental and Molecular Mechanisms of Mutagenesis* 614.1 (2007). Cell type specificity in DNA damage response, pp. 16–23. ISSN: 0027-5107. DOI: https://doi.org/10.1016/j.mrfmmm.2006.06.005 (cit. on p. 10).

[79] P. Fortini et al. "DNA damage response by single-strand breaks in terminally differentiated muscle cells and the control of muscle integrity". In: *Cell death and differentiation* 19 (2012-06), pp. 1741–9. DOI: 10.1038/cdd.2012.53 (cit. on p. 10).

[80] W. Schmidt et al. "DNA Damage, Somatic Aneuploidy, and Malignant Sarcoma Susceptibility in Muscular Dystrophies". In: *PLoS genetics* 7 (2011-04), e1002042. DOI: 10.1371/journal.pgen.1002042 (cit. on pp. 10, 11).

[81] B. Liu et al. "Genomic instability in laminopathy-based premature aging". In: *Nature medicine* 11 (2005-08), pp. 780–5. DOI: 10.1038/nm1266 (cit. on p. 10).

[82] T. Zhang et al. "Net39 protects muscle nuclei from mechanical stress during the pathogenesis of Emery-Dreifuss muscular dystrophy". In: *Journal of Clinical Investigation* 133 (2023-07). DOI: 10.1172/JCI163333 (cit. on p. 10).

[83] S. A. Richards et al. "The accumulation of un-repairable DNA damage in laminopathy progeria fibroblasts is caused by ROS generation and is prevented by treatment with N-acetyl cysteine". In: *Human Molecular Genetics* 20.20 (2011-08), pp. 3997–4004. ISSN: 0964-6906. DOI: 10.1093/hmg/ddr327 (cit. on p. 11).

[84] Y. Bou Saada et al. "Facioscapulohumeral dystrophy myoblasts efficiently repair moderate levels of oxidative DNA damage". In: *Histochemistry and Cell Biology* 145 (2016-04). DOI: 10.1007/s00418-016-1410-2 (cit. on p. 11).

[85] P. Dmitriev et al. "DUX4-induced constitutive DNA damage and oxidative stress contribute to aberrant differentiation of myoblasts from FSHD patients". In: *Free Radical Biology and Medicine* 99 (2016), pp. 244–258. ISSN: 0891-5849. DOI: https://doi.org/10.1016/j.freeradbiomed.2016.08.007 (cit. on p. 11).

[86] G. Togliatto et al. "Unacylated Ghrelin Promotes Skeletal Muscle Regeneration Following Hindlimb Ischemia via SOD-2–Mediated miR-221/222 Expression". In: *Journal of the American Heart Association* 2 (2013-10), e000376. DOI: 10.1161/JAHA.113.000376 (cit. on p. 11).

[87] M. Hidalgo et al. "Oxygen Modulates the Glutathione Peroxidase Activity during the L6 Myoblast Early Differentiation Process". In: *Cellular Physiology and Biochemistry* 33.1 (2014-01), pp. 67–77. ISSN: 1015-8987. DOI: 10.1159/000356650 (cit. on p. 11).

[88] A. Bosutti and H. Degens. "The impact of resveratrol and hydrogen peroxide on muscle cell plasticity shows a dose-dependent interaction". In: *Scientific Reports* 5 (2015) (cit. on p. 11).

[89] M. Hansen, D. Rubinsztein, and D. Walker. "Autophagy as a promoter of longevity: insights from model organisms." In: (2018-07). DOI: 10.17863/CAM.25782 (cit. on p. 11).

[90] A. R. Winslow et al. "-Synuclein impairs macroautophagy: implications for Parkinson's disease". In: *Journal of Cell Biology* 190.6 (2010-09), pp. 1023–1037. ISSN: 0021-9525. DOI: 10.1083/jcb.201003122 (cit. on p. 11).

[91] T. Noda and Y. Ohsumi. "Tor, a Phosphatidylinositol Kinase Homologue, Controls Autophagy in Yeast*". In: *Journal of Biological Chemistry* 273.7 (1998), pp. 3963–3966. ISSN: 0021-9258. DOI: https://doi.org/10.1074/jbc.273.7.3963 (cit. on p. 11).

[92] D. Meley et al. "AMP-activated Protein Kinase and the Regulation of Autophagic Proteolysis*". In: *Journal of Biological Chemistry* 281.46 (2006), pp. 34870–34879. ISSN: 0021-9258. DOI: https://doi.org/10.1074/jbc.M605488200 (cit. on p. 11).

[93] A. Petiot et al. "Distinct Classes of Phosphatidylinositol 3-Kinases Are Involved in Signaling Pathways That Control Macroautophagy in HT-29 Cells*". In: *Journal of Biological Chemistry* 275.2 (2000), pp. 992–998. ISSN: 0021-9258. DOI: https://doi.org/10.1074/jbc.275.2.992 (cit. on p. 11).

[94] V. Kanamarlapudi. "Centaurin-1 and KIF13B kinesin motor protein interaction in ARF6 signalling". In: *Biochemical Society Transactions* 33.6 (2005-10), pp. 1279–1281. ISSN: 0300-5127. DOI: 10.1042/BST0331279 (cit. on p. 11).

[95] Y. Kabeya et al. "LC3, a mammalian homologue of yeast Apg8p, is localized in autophagosome membranes after processing". In: *The EMBO Journal* 19.21 (2000), pp. 5720–5728. DOI: https://doi.org/10.1093/emboj/19.21.5720 (cit. on p. 12).

[96] Z. Yang and D. J. Klionsky. *An overview of the molecular mechanism of autophagy*. 2009. DOI: 10.1007/978-3-642-00302-8_1 (cit. on p. 12).

[97] P. Roberts et al. "Piecemeal Microautophagy of Nucleus in Saccharomyces cerevisiae". In: *Molecular biology of the cell* 14 (2003-02), pp. 129–41. DOI: 10.1091/mbc.E02-08-0483 (cit. on p. 12).

[98] T. Akematsu, R. E. Pearlman, and H. Endoh. "Gigantic macroautophagy in programmed nuclear death of Tetrahymena thermophila". In: *Autophagy* 6 (7 2010-10), pp. 901–911. ISSN: 15548635. DOI: 10.4161/auto.6.7.13287 (cit. on p. 12).

[99] J.-y. Shoji et al. "Macroautophagy-Mediated Degradation of Whole Nuclei in the Filamentous Fungus Aspergillus oryzae". In: *PLOS ONE* 5.12 (2010-12), pp. 1–6. DOI: 10.1371/journal.pone.0015650 (cit. on p. 12).

[100] S. Rello-Varona et al. "Autophagic removal of micronuclei". In: *Cell cycle (Georgetown, Tex.)* 11 (2012-01), pp. 170–6. DOI: 10.4161/cc.11.1.18564 (cit. on p. 12).

[101] K. Mamchaoui et al. "Immortalized pathological human myoblasts: towards a universal tool for the study of neuromuscular disorders." In: *Skeletal Muscle* 1.1 (2011-11), p. 34. DOI: 10.1186/2044-5040-1-34. URL: https://inserm.hal.science/inserm-00651121 (cit. on p. 15).

[102] B. M. Freyter et al. "Nuclear Fragility in Radiation-Induced Senescence: Blebs and Tubes Visualized by 3D Electron Microscopy". In: *Cells* 11.2 (2022). ISSN: 2073-4409. DOI: 10.3390/cells11020273 (cit. on p. 41).

[103] J.-H. Lee et al. "Modulation of proliferation and differentiation of C2C12 skeletal muscle cells by fatty acids". In: *Life Sciences* 84.13 (2009), pp. 415–420. ISSN: 0024-3205. DOI: https://doi.org/10.1016/j.lfs.2009.01.004 (cit. on p. 42).

[104] A. Zetser, E. Gredinger, and E. Bengal. "p38 Mitogen-activated Protein Kinase Pathway Promotes Skeletal Muscle Differentiation: PARTICIPATION OF THE MEF2C TRANSCRIPTION FACTOR*". In: *Journal of Biological Chemistry* 274.8 (1999), pp. 5193–5200. ISSN: 0021-9258. DOI: https://doi.org/10.1074/jbc.274.8.5193 (cit. on p. 42).

[105] M. Girven et al. "l-glutamine Improves Skeletal Muscle Cell Differentiation and Prevents Myotube Atrophy After Cytokine (TNF-) Stress Via Reduced p38 MAPK Signal Transduction". In: *Journal of Cellular Physiology* 231.12 (2016), pp. 2720–2732. DOI: https://doi.org/10.1002/jcp.25380 (cit. on p. 43).

[106] O. D. Perez et al. "Inhibition and Reversal of Myogenic Differentiation by Purine-Based Microtubule Assembly Inhibitors". In: *Chemistry Biology* 9.4 (2002), pp. 475–483. ISSN: 1074-5521. DOI: https://doi.org/10.1016/S1074-5521(02)00131-X (cit. on p. 43).

[107] D. M. Valenzuela et al. "Receptor tyrosine kinase specific for the skeletal muscle lineage: Expression in embryonic muscle, at the neuromuscular junction, and after injury". In: *Neuron* 15.3 (1995), pp. 573–584. ISSN: 0896-6273. DOI: https://doi.org/10.1016/0896-6273(95)90146-9 (cit. on p. 43).

[108] T. Fiaschi et al. "Low Molecular Weight Protein-tyrosine Phosphatase Is Involved in Growth Inhibition during Cell Differentiation*". In: *Journal of Biological Chemistry* 276.52 (2001), pp. 49156–49163. ISSN: 0021-9258. DOI: https://doi.org/10.1074/jbc.M107538200 (cit. on p. 43).

[109] S. L. Chen et al. "The Coactivator-associated Arginine Methyltransferase Is Necessary for Muscle Differentiation: CARM1 COACTIVATES MYOCYTE ENHANCER FACTOR-2*". In: *Journal of Biological Chemistry* 277.6 (2002), pp. 4324–4333. ISSN: 0021-9258. DOI: https://doi.org/10.1074/jbc.M109835200 (cit. on p. 43).

[110] H.-J. Jeong et al. "Prmt7 promotes myoblast differentiation via methylation of p38MAPK on arginine residue 70". In: *Cell Death Differentiation* 27 (2019-06). DOI: 10.1038/s41418-019-0373-y (cit. on p. 43).

[111] M. Sandri et al. “Myoblasts and myotubes in primary cultures deprived of growth factors undergo apoptosis”. In: *Basic Appl. Myol.* 6 (1996), pp. 257–260 (cit. on p. 44).

[112] K. Koishi et al. “MyoD protein accumulates in satellite cells and is neurally regulated in regenerating myotubes and skeletal muscle fibers”. In: *Developmental Dynamics* 202 (1995). URL: https://api.semanticscholar.org/CorpusID:7507864 (cit. on p. 46).

I

Methods specification

I.1 Experimental settings

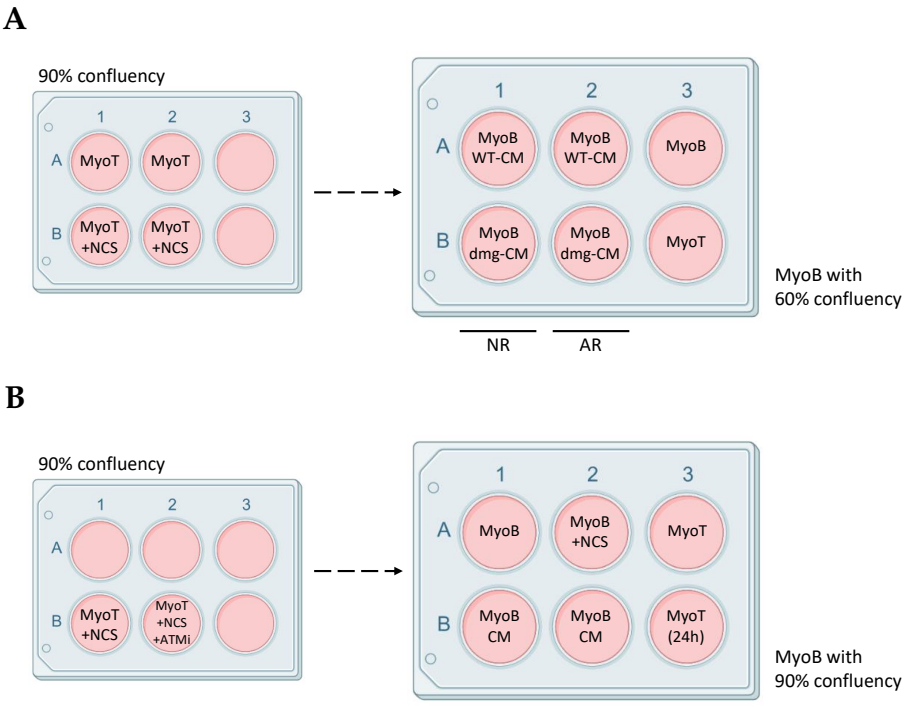

Figure I.1: Experimental setting of the analysis of MyoB treated with CM. (A) MyoB were differentiated with a 90% confluency during 5 days. Half the conditions were incubated with 0.5 μL of 2.5 μM of NCS for 30 min. The conditioned mediums were added to a new plate with MyoB with a 60% confluency, where half the conditions had the same medium since the first day (NR) while the rest had their medium renewed every day (AR). The medium was being renewed with fresh CM from the treated plate. Differentiation was induced to one well containing MyoB. **(B)** MyoB at 90% confluency were incubated with NCS (same quantity as before) and one of them was also treated with 1 μL of 2.5 μM of ATMi. The CM were added to MyoB with a 90% confluency. In that plate, we also included the following controls: MyoB treated with NCS and MyoT differentiated for 24 h or 5 days.

I.2 Parameters selected for UPLC-MS analysis

Table I.1: Parameters selected for UPLC-MS analysis of damaged Myot CM metabolites.

Mass scan mode		
Full Scan		
m/z	70-1050	
Resolution	70,000	
dd-MS2		
TopN	10	
Resolution	17,500	
Collision mode	HCD	
Mass spectrometry parameters	ESI+	ESI-
Heater Temp (ºC)	300	
Sheath Gas Flow rate (arb)	45	
Aux Gas Flow Rate (arb)	15	
Sweep Gas Flow Rate (arb)	1	
Spray voltage (kV)	3.0	3.2
Capillary Temp (ºC)	350	
S-Lens RF Level (%)	30	60

I.3 Composition of running and stacking gel used for WB

Table I.2: Composition of the 6% and 12% bis-acrylamide running gel used for the Western Blot. The volume presented allows the preparation of 2 gels.

SDS-PAGE running gel - 2 gels	Volume (mL)	
	6% Gel	12% Gel
H2O	6	4.5
R-gel buffer	2.5	
40% Bis-Acrylamide (NZYTech)	1.5	3
	Volume (μL)	
TEMED (Sigma Life Science)	40	
APS 10%	20	

Table I.3: Composition of the bis-acrylamide stacking gel used for the Western Blot. The volume presented allows the preparation of 2 gels.

SDS-PAGE stacking gel - 2 gels	Volume (mL)
H2O	5
S-gel buffer	2
40% Bis-Acrylamide (NZYTech)	0.9
	Volume (μL)
TEMED (Sigma Life Science)	40
APS 10%	40

I.4 Cycle steps parameters and sequence of primers used for RT-qPCR analysis

Table I.4: Cycle steps parameters for RT-qPCR analysis of differentiation marker identification and MyoB response to damaged MyoT CM.

RT-qPCR cycle steps	Steps	Temperature (ºC)	Time (min)	Number of cycles
Hold	1	50	2	1
	2	95	2	
PCR	1	95	0:15	40
	2	60	1	
Melt curve	1	95	0:15	1
	2	60	1	
	3	95	0:15	

Table I.5: Sequence of primers used for RT-qPCR analysis of differentiation marker identification and MyoB response to damaged MyoT CM.

Gene	Forward Primer (5′-3′)	Reverse Primer (5′-3′)
DES	TCG GCT CTA AGG GCT CCT C	CGT GGT CAG AAA CTC CTG GTT
MYOD1	CCG CTT TCC TTA ACC ACA AAT C	CGG CTG TAG ATA GCA AAG TGC
MYOG	GTG CCA TCC AGT ACA TCG AGC C	CCC GGC TTG GAA GAC AAT CT
MYH3	ATT GCT TCG TGG TGG ACT CAA	GGC CAT GTC TTC GAT CCT GTC
DYSF	CTG TCG CAA GCC TGA CTT T	CGT CTC ATG GTC TTT GAC CAC

I.5 Laser parameters used for IF analysis

Table I.6: Laser parameters used for IF analysis of differentiation marker identification and MyoB response to damaged MyoT CM.

	Track 1	Track 2	
Detection wavelength	642-755	410-504	
Laser power percentage (%)	3.0	1.2	
Laser wavelength	633	405	
	channel 1	channel 2	channel 3
Detection gain	700	625	358

II

Additional results

II.1 Images of WT MyoT

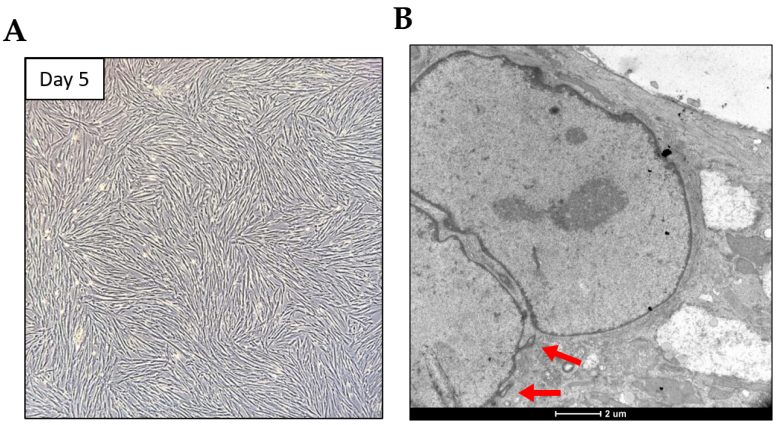

Figure II.1: Images of WT MyoT obtained by optical and electronic microscopy. (A) Photos taken by an optical microscope with a 4x objective of MyoT cell culture terminally differentiated (day 5). **(B)** Images obtained by EM show WT differentiated KM155 cell line. The image shows the nuclear membrane and respective protrusions highlighted by red arrows.

II.2 Analysis of WT MyoT and MyoT treated with NCS by WB

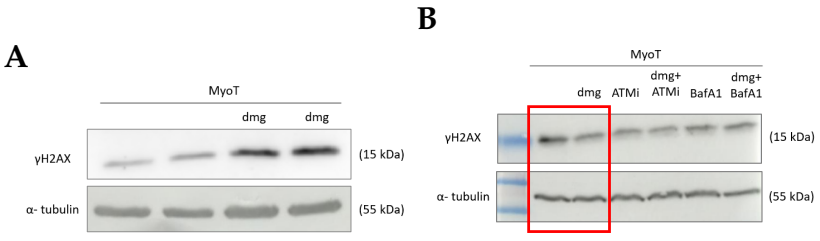

Figure II.2: MyoT treated with NCS do not present the same levels of DNA damage. WB of WT MyoT and MyoT treated with NCS with a 90% confluency (in **(B)** it is highlighted in red). The same drug sample was used to damage the MyoT which was developed the CM to the MyoB in **(A)** Figure 3.9**A** and **(B)** Figure 3.9**B**. The analysis was made against γH2AX protein expression (12% running gel) and α-tubulin was used as the loading control protein.